Institute for Anatomy and Cell Biology

Director Prof. Dr. med. Tobias M. Böckers

Characterization of a novel GFP-SHANK3 transgenic mouse model of autism spectrum disorders

Dissertation to achieve the medical doctoral degree of the medical faculty of Ulm University

Kevin Thome

Munich

2019

Current dean of faculty: Prof. Dr. T. Wirth

1. Supervisor: Prof. Dr. T. Boeckers
2. Supervisor : PD Dr. S. Jesse

Day doctorate awarded: 7.7.2022

Contents

Abbreviations (in alphabetical order)

AB = antibody

ADHD = attention deficit hyperactivity disorder

ALS = amyotrophic lateral sclerosis

ASD = autism spectrum disorder

BSA = bovine serum albumin

CaM kinase II = Ca^{2+}/calmodulin-dependent protein kinase II

cat.no. = catalog number

CortBP = cortactin binding protein

Cre = causes recombination

dSTORM = direct stochastical optical reconstruction microscopy

EEG = electroencephalography

EGFP = enhanced green fluorescent protein

ExM = expansion microscopy

floxing = flanked by loxP

GFP = green fluorescent protein

GS3 = GFP-Shank3

Ho = homogenate

kDa = kilodalton

LM = light membranes

LoxP= locus of X-over P1

M = molar

mM = millimolar

Mit = mitochondrium

MW = molecular weight

Myl = myelin

nm = nanometer

P1-3 = pellet 1-3

P20-21 = postnatal days 20-21

PBS = phosphate buffered saline

PDZ = PSD-95, Drosophila disc large tumor suppressor, zona occludens 1

PFA = paraformaldehyde

ProSAP = proline-rich synapse-associated protein

PSD = postsynaptic density

RT = room temperature

S1-3 = supernatant 1-3

SAM = sterile alpha motif

SH3 = SRC homology 3 domain

SHANK3 = SH3 and multiple ankyrin repeat domains 3

SSTRIP = somatostatin-receptor-interacting protein

STED = stimulated emission depletion

Syn = synaptosome

TBK1 = TANK-binding kinase 1

ter = terminal

tet = tetracycline

TFZ = Tierforschungszentrum

WB = western blot

Wt = wildtype

1. Introduction

This thesis deals with the characterization of a new mouse model in the setting of an artificial protein overexpression. The protein of interest is a synaptic protein called SH3 and multiple ankyrin repeat domains 3 (SHANK3) and it is associated with autism spectrum disorder (ASD). In this setting it is overexpressed as a fusion protein with an N-terminally positioned green fluorescent protein (GFP). We refer to these transgenic mice as 'GFP-SHANK3' mice.

1.1 Autism spectrum disorders

1.1.1 Diagnostic criteria

In the year 2013 the fifth edition of the 'Diagnostic and Statistical Manual of Mental Disorders' changed the diagnostic criteria of autism disorders. In the fourth edition there were four different disorders one could be diagnosed with: (1) autistic disorder (2) Asperger's disorder (3) childhood disintegrative disorder, and (4) pervasive developmental disorder. The fifth edition introduces an umbrella term coined 'Autism spectrum disorder' (american psychiatric association, DSM – 5 fact sheet, autism spectrum disorder, page 1). This term should encompass the four previous terms as well as incorporate the many variations of phenotypes that share a common pattern. The main features of ASD are (1) limited and stereotypical patterns of activities and interests, as well as (2) deficits in social communication and interaction (american psychiatric association, DSM – 5 fact sheet, autism spectrum disorder). Other defects such as hyperactivity (Nickl-Jockschat and Michel 2011), epilepsy (Tuchman and Rapin 2002) or intellectual disability (Amaral et al. 2008) also often occur.

1.1.2 Epidemiology

According to the latest large scale surveys the prevalence of ASD is about 1% - 2% (Park et al. 2016) with a male to female ratio of about 4.3 to 1 (Lai et al. 2012). The differences in the expression of phenotypes, as well as the differences in their severity seem to fit with the fact that there is no single cause for ASD. Instead, the current opinion is that there is a broad range of factors that play a part in its development. Some of them are the result of genetic risk factors and others of non-genetic risk factors. Of all ASD cases, those with a background range from 10% - 20%. The rest are mainly due to external factors (Park et al. 2016).

1.2 The Shank protein

1.2.1 Synonyms

In order to avoid potential confusion in process of researching it could be helpful to note the following: In the year 1999 there were seven groups that discovered this family of proteins more or less simultaneously. Hence, there were different synonyms for it, namely (1) Synamon, (2) ProSAP, (3) CortBP, (4) Spank, and (5) SSTRIP (Sheng and Kim 2000). However, the name SHANK has established itself since then, which is why this thesis will solely refer to it as such.

1.2.2 Genes

There are three genes coding for the SHANK Proteins: *SHANK1*, *SHANK2* and *SHANK3*. Despite the fact that there are only three genes, an elaborate number of different possibilities for alternative splicing and intragenic promotors (Jiang and Ehlers 2013) yields a large variety of different proteins stemming from them (Boeckers et al. 1999a, Lim et al. 1999).

1.2.3 Function & Localization

The main function of the SHANK proteins is that of a scaffold protein (Sheng and Kim 2000). Regarding their localization: (1) The mRNA of SHANK1 was found virtually nowhere but in the brain. (2) That of SHANK2 was found mostly in the brain, but also in the kidneys and in the liver, and (3) SHANK3 mRNA was found mostly in the heart while in lower levels in the brain and the spleen. (Lim et al. 1999). Although the SHANK proteins are mainly localized at the postsynaptic density (Naisbitt et al. 1999) of excitatory neurons specifically (Naisbitt et al. 1999, Tu et al. 1999, Boeckers et al. 1999a). There is also a more recent paper which found them to play a role in axons (Halbedl et al. 2016). Within the postsynaptic density the SHANK protein is generally localized evenly, but with a stronger concentration at the proximal/cytoplasmic end (Naisbitt et al. 1999). There it resides at the transition point between the density of the membranous molecules and the proteins of the cytoskeleton, and therefore hinting at a potential role in connecting the glutamate receptors at the synapse to the structure of the cell (Sala et al. 2001).

1.2.4 Structure

The basic structure of the *SHANK* gene codes for five parts: N-terminal - (1) ankyrin repeats, (2) an SH3 domain, (3) a PDZ domain, (4) a long proline-rich region, and (5) a SAM domain - C-terminal (Sheng and Kim 2000). All of these can take part in protein-protein interactions, highlighting the important structural role of this protein as a scaffolding protein. The large splicing products are roughly 2000 amino acids in length and over 200 kDa heavy (Sheng and Kim 2000).

1.2.5 Functions of the domains

In order to give a more detailed impression of the SHANK proteins functions, here are some examples of the functions of its domains: (1) The ankyrin repeats interact with α-fodrin, (a

protein of the membrane-cytoskeleton) (Böckers et al. 2001) and sharpin (a PKC-binding protein) (Lim et al. 2001). (2) The exact function of the SH3 domain is not known at this point. SH3 domains from other proteins (such as Abil) bind to proline-rich regions. However, even though the SHANK3-SH3 domain is structurally quite similar, it lacks certain peptide binding residues of canonical SH3 domains. Currently entertained hypotheses are that it might have specific binding partners yet to be found, that it influences the binding properties of the neighboring PDZ domain or that it has simply lost its function in the course of evolution (Ponna et al. 2017). (3) The PDZ domain interacts with SAPAP (a.k.a. GKAP, another scaffolding protein) (Naisbitt et al. 1999), CIRL-1 (a G-protein-coupled receptor) (Kreienkamp et al. 2000), SSTR2 (somatostatin receptor 2, also a G-protein-coupled receptor) (Zitzer et al. 1999) and others. (4) The proline-rich region binds Homer (an adaptor protein) (Tu et al. 1999), cortactin (a regulator of the actin cytoskeleton) (Naisbitt et al. 1999), Abp1 (a protein that binds actin) (Qualmann et al. 2004) and IRSp53 (a substrate of the insulin receptor) (Bockmann et al. 2002, Soltau et al. 2002). (5) The SAM domain interacts with other SAM domains, enabling the SHANK proteins to multimerize and form helical fibers, which in turn form large structures that have a sheet-like appearance (Baron et al. 2006).

1.3 Connection between autism and the SHANK protein

There are hundreds of genes associated with ASD. One group of these genes is that of the synaptic proteins (Betancur 2011). Examples of such synaptic proteins are those of the SHANK family.

1.3.1 Epidemiology

Of all ASD cases, *SHANK* mutations are responsible for roughly 1% (Leblond et al. 2014). *SHANK1* mutations account for 0.04%, *SHANK2* mutations for 0.17% and *SHANK3* mutations for 0.69% of all ASD cases (Leblond et al. 2014). Not only is the *SHANK3* mutation the most common out of the three, but its symptoms are also the most severe (Leblond et al. 2014). It has

therefore been suggested that *SHANK* mutations alone may be a monogenetic cause of ASD and should hence be considered for screening in clinical practice. SHANK3 is in fact currently seen as the most crucial gene in a genetic disorder called Phelan-McDermid-Syndrome, a.k.a. 22q13.3 deletion syndrome, a subtype of ASD (Kolevzon et al. 2014).

1.3.2 Phenotypes of SHANK disorder models

(1) SHANK1: (1.1) *Shank1*-knockout animals show increased anxiety, decreased vocal communication, decreased locomotion and - remarkably - enhanced working memory, but decreased long term memory (Wöhr et al. 2011, Leblond et al. 2014). (1.2) Mouse models of SHANK1 overexpression have not been published to this date. Results on SHANK1 overexpression in cultured hippocampal neurons, however, are available. They show an enlargement of dendritic spines with a lower overall density (Sala et al. 2001). (2) SHANK2: (2.1) *Shank2*-knockout animals show hyperactivity, increased anxiety, repetitive grooming, and abnormalities in vocal and social behaviors (Berkel et al. 2010, Schmeisser et al. 2012, Won et al. 2012). (2.2) Just as for SHANK1 overexpression, there are no animal models for SHANK2. But again, there are cell culture experiments with primary hippocampal neurons overexpressing SHANK2 which show an increase in the volume of dendritic spines (Berkel et al. 2012). (3) SHANK3: (3.1) *Shank3*-knockout animals show self-injurious and repetitive grooming as well as deficits in social interaction and communication (Durand et al. 2007, Peça et al. 2011, Wang et al. 2011, Yang et al. 2012). (3.2) *Shank3*-knockin animals show manic-like behavior, epileptic seizures, hyperkinetic disorders and anxiety. In contrast to the *Shank3*-knockout animals however, there is no repetitive behavior (Han et al. 2013, Mei et al. 2016). There are also models of SHANK3 deficiency in rats as well as in primates. The SHANK3 deficient rats displayed decreased vocalization and social interaction (Berg et al. 2018). Regarding the SHANK3 deficient primates, it must be mentioned that there was no official publication, but instead a letter to the author. In it, the primates were only examined *post mortem*. The first observation was that the pregnancy rates were very low. Also, out of 116 injected embryos, merely one offspring was born alive. This suggests that maybe SHANK3 plays an important role in the early development of non-human primates. Temporal expression patterns of different SHANK3

isoforms are different in primates than in mice. This also suggests that the functions of the different SHANK3 isoforms may have changed in the course of evolution. Furthermore, there were findings that were consistent with previous findings in rodents, e.g. reduced spine density. However, there were also findings that differed from rodents, such as fewer NeuN+ neurons and more GFAP+ astrocytes in the prefrontal cortex. This supports the idea of the evolutionary development of unique SHANK3 functions in the brain of non-human primates (Zhao et al. 2017a).

1.4 The mouse model

1.4.1 The analyzed mouse model

The species of the mouse is Mus Musculus domesticus and the line is C57BL/6J. This species and this line were chosen, because they are common for experiments involving gene manipulation. So for one, there are a lot of known methods established and known to work in the context of this animal strain. Additionally, using a mouse line that is more commonly used by the scientific community provides more comparability of our results with published work.

1.4.2 Targeting construct

This model was developed by Mr. Prof. Dr. Jürgen Bockmann from the Institute of Anatomy and Cell Biology of Ulm University. He kindly provided figure 1, which shows a schematic overview of the targeting construct. The targeting construct consists of two genes that share a bidirectional promoter. One of the genes codes for luciferase, a reporter enzyme that produces bioluminescence and which was isolated from fireflies in 1987 (de Wet et al. 1987, Gould and Subramani 1988). The other gene codes for a fusion protein consisting of SHANK3 and - attached to its N-terminus - a green fluorescent protein. The construct was inserted in the so called ‘Rosa26 Locus’. The Rosa26 Locus was discovered when developing gene trapping vectors in embryonic stem cells of mice (Friedrich and Soriano 1991). The gene is suspected to

code for at least 3 transcripts of unknown function (Zambrowicz et al. 1997). However, known insertions into this region have so far not produced any relevant phenotypes. The promoter of the targeting construct needs to bind a transactivator in order to be active.

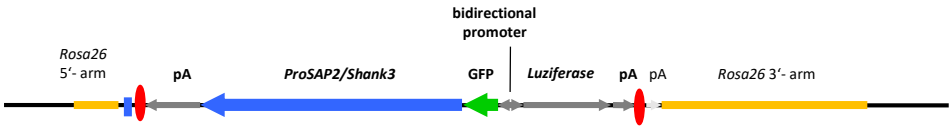

Figure 1: Targeting construct of the transgenic mouse. GFP = green fluorescent protein; pA = poly-A; = attachment site; = loxP. This figure was kindly provided by Mr. Prof. Dr. Jürgen Bockmann (Institute for Anatomy and Cell Biology of Ulm University)

1.4.3 Transactivator

The transactivator itself is coded by another gene whose expression is controlled by a CaM kinase II promoter. The Protein CaM kinase II was discovered in 1981 and then isolated and characterized in 1983 where it was shown to be highly enriched in neurons of the brain (Kennedy and Greengard 1981, Kennedy et al. 1983, Bennett et al. 1983) and within the brain especially in the forebrain (Wang et al. 2013). This means, that even though the transactivator gene of course exists ubiquitously in the organism of the animal, it is only expressed in neurons of the forebrain. Now since the targeting construct needs this transactivator in order to be active, this in turn means that the fusion protein is also only expressed in neurons of the brain.

1.4.4 Tet-off system

The tet-system was first introduced in 1992 (Gossen and Bujard 1992). In this context 'tet' stands for 'tetracycline', a group of antibiotics. Of this group of antibiotics, the model of this thesis responds to doxycycline specifically. The tet-off system generally is a system in which the presence of a tetracycline inhibits its function. So in this system specifically, (1) doxycycline

binds to the transactivator, (2) which makes the transactivator unable to bind to the promoter of the fusion protein, (3) and therefore inhibits the transcription of said fusion protein.

1.4.5 Han et al., 2013

Since the group of Han et al. experiments with SHANK3 overexpressing mice as well, it is worthwhile to elaborate on their findings.

Transfection

This group used a BAC-clone to inject DNA, coding for an enhanced green fluorescent protein (EGFP-Shank3), in front of one of the physiological *Shank3* genes. This was done with embryos of a mouse line called 'FVB/N' (Han et al. 2013).

Localization

The group of Han et al. found *EGFP-Shank3* transcripts mainly in cortex, hippocampus and striatum, which is similar to the localization of endogenous SHANK3. Also similar to endogenous Shnak3, cell culture experiments found EGFP-SHANK3 to be mostly in the spines of dendrites, and there co-localizing with PSD-95 (an excitatory, postsynaptic marker), but not with gephyrin (an inhibitory, postsynaptic marker) (Han et al. 2013).

Overexpression

With western blots they showed that their transgenic mice expressed 1.2 times as much SHANK3 of each isoform as the wildtypes do. Furthermore, the blots also showed, that the transgenic mice express 50% more overall SHANK3, which matches the levels of human patients with *SHANK3* duplications (Han et al. 2013).

Behavior

Many behavioral tests were done in this study of which I will not list all of the findings here. It can be concluded however that summarized, they result in a phenotype that is hyperkinetic and decreased in social interaction. Also, in contrast to *Shank3*-knockout animals, they did not engage in repetitive behavior. They further state that all of this resembles the behavior of a human during a manic episode. One other phenotype worth mentioning was the occurrence of spontaneous seizures. The study writes that the behavioral findings are very comparable to patients that the group found, who have *SHANK3* duplications leading to 22q13 trisomies (Han et al. 2013).

Pharmaceutical Treatment

To further test the resemblance to human conditions they tested three pharmaceutical drugs: (1) amphetamines, (2) lithium and (3) valproate. The amphetamines are used for treating ADHD in humans, were they paradoxically act calming. In the transgenic mice, the amphetamines did not lead to this paradoxical calming effect, but instead to an increase of the hyperactivity. This fits to the way amphetamines act in human patients with mania. Lithium is used for the treatment of bipolar disorder in humans and valproate treats mania, mixed episodes and convulsions. Lithium did not lessen the mania in the transgenic mice. Valproate did help with some of the symptoms and also decreased the frequency of the seizures. It can thus far be concluded that the findings of the pharmaceutical treatment further facilitate the suspicion of mania in the transgenic mice (Han et al. 2013).

Rescue

By crossing the transgenic mice with *Shank3*$^{+/-}$-mice, many of the symptoms observed in the transgenic mice were reversed (Han et al. 2013).

1.5 Aims of the thesis

The aims of this thesis regard two projects: (1) the characterization of the new GFP-SHANK3 mouse model. In the future, it should hopefully enable us to broaden our understanding of ASD in more detail, by modeling SHANK3 overexpression. (2) The establishing of the new expansion microscopy method.

1.5.1 The GFP-SHANK3 mouse model

Broadly stated, the goal of this project is to establish the new mouse model. This means concretely: To show (1) that the mice express the GFP-SHANK3 fusion protein in the first place, (2) that it is located where a CaM kinase II - specific promoter would lead to its expression and (3) that it is located where natural SHANK3 is located, namely the postsynaptic density. The methods used are western blotting and immunohistochemistry.

1.5.2 Expansion microscopy

The goal of this project is to establish the new expansion microscopy method in the laboratory of the Institute for Anatomy and Cell Biology of Ulm University.

2. Materials & Methods

2.1 Materials

2.1.1 Mice

The species of the animal is ‘Mus Musculus domesticus’. The line C57BL/6J was obtained from Janvier. The line B6.Cg-Tg(Camk2a-tTA)1Mmay/DboJ (expresses the transactivator) stems from Dr. Bernd Baumann (Institute for Physiological Chemistry, Ulm University) and is also being held by Prof. Dr. Tobias M. Boeckers in the TFZ Oberberghof. The transactivator of that mouse was crossbred into a line which is now called ‘B6.Rosa26tm1(tetO-EGFP-Prosap2)Tmb/N’. This was done by the group of Dr. Bockmann, in the Biocenter Oulu of Oulu University in Finnland as well as by the group of Dr. Jürgen Bockmann in the institute for anatomy and cell biology of Ulm University. The number of the animal experiment application is 1252.

2.1.2 Antibodies

2.1.2.1 For western blot

primary antibodies

- mouse anti GFP: Clontech, cat.no. 632381
- rabbit anti SHANK3: self made

- mouse anti PSD-95: abcam, cat.no. ab2723
- mouse anti beta-actin: Sigma-Aldrich, cat.no. A5316

secondary antibodies

- Polyclonal goat anti rabbit antibody: DAKO, cat.no. D0487
- Polyclonal rabbit anti mouse antibody: DAKO cat.no. D0314

2.1.2.2 For immunohistochemistry

primary antibodies

- mouse anti GFP: Clontech, cat.no. 632381
- guinea pig anti MAP2: Synaptic Systems, cat.no. 188004
- mouse anti bassoon: Enzo, cat.no. ADI-VAM-PS003
- rabbit anti SHANK3: self-made

secondary antibodies

- anti mouse 488
- anti rabbit 488
- anti guinea pig 568
- anti mouse 568
- anti rabbit 647
- anti mouse 647

➔ all the secondary antibodies were acquired from Thermo Fisher Scientific, Eugene, USA

2.1.3 Chemicals

- Albuminfraktion V (pH 7,0) for molecular biology (BSA): BioFroxx, cat.no. 1126
- Ammonium Persulfat (APS; (NH4)2S2O8): Sigma-Aldrich, cat.no. A3678
- Bis (N,N‘-Methylenbisacrylamid): Sigma-Aldrich, cat.no. M7279
- Bromphenol blue (3′,3″,5′,5″-Tetrabromophenolsulfonephthalein): Sigma-Aldrich, cat.no. B0126
- complete, EDTA-free Protease Inhibitor Cocktail: Sigma-Aldrich, cat.no. 04693132001
- Di-Sodiumhydrogenphosphat-Dihydrat (Na2HPO4x2H2O): Applichem, cat.no. A3905,1000
- DTT (1,4-Dithiothreitol): Sigma-Aldrich, cat.no. DTT-RO
- EDTA (Ethylenediaminetetraacetic acid): Sigma-Aldrich, cat.no. EDS-100G
- Glycin: NeoFroxx, cat. no. LC-4522Sodium-Chloride (NaCl): Honeywell, cat.no. 31434
- Guanidin-Hydrogen-Chloride : Carl Roth, cat.no. 0037
- HEPES (N-2-Hydroxyethylpiperazin-N'-2-ethansulfonsäure): Carl Roth, cat.no. 9105
- Paraformaldehyd (PFA): Sigma-Aldrich, cat.no. P6148
- Potassium-Chloride (KCl): Carl Roth, cat.no. 6781
- Potassium-Dihydrogen-Phosphate (KH2PO4): Merck, cat.no. 1048730250
- SDS (Sodium dodecyl sulfate): Carl Roth, cat.no. 8029
- Serva Blue G: Serva, cat.no. 35050
- Skim Milk Powder: Sigma-Aldrich, cat.no. 70166
- Sodium Chloride (NaCl): Honeywell, cat.no. 31434
- Saccharose (Sucrose): Carl Roth, cat.no. 4621
- Tris for molecular biology (2-Amino-2-Hydroxymethyl-1,3-Propanediol): Applichem, cat.no. A2264
- Tris-HCl (Tris-(hydroxymethyl)-aminomethanhydrochlorid): Carl Roth, cat.no. 9090

2.1.4 Solutions

- Acrylamide/Bis Solution, 29:1: Serva, cat.no. 10687
- Acrylamide Solution 40 %: Biorad, cat.no. 1610140
- DAPI (4',6-Diamidino-2-Phenylindole, Dihydrochloride): Thermo-Fischer, cat.no. D1306
- Ethanol (CH3CH2OH): Honeywell, cat.no. 32205
- Glycerol (1,2,3-Propanetriol): Honeywell, cat.no. 15523
- Hydrochloric Acid Solution (HCl): Honeywell, cat.no. 35328
- Ketamine: Wirtschaftsgenossenschaft deutscher Tierärzte
- Phosphoric Acid: VWR, cat.no. 20624
- Pierce ECL western blotting Substrate: Thermo-Fischer, cat.no. 32106
- Sodium Chloride Solution 0.9 %: Sigma-Aldrich, cat.no. S8776
- Sodium Hydroxide (NaOH): VWR, cat.no. 470302
- TransBlot®Turbo™ 5x Trasnfer Puffer: Biorad, cat.no. 10026938
- Triton X-100: Sigma-Aldrich, cat.no. 10789704001
- Tissue-Tek O.C.T. Compound: Sakura, cat.no. 4583
- TWEEN 20 (Polyoxyethylene (20) sorbitan monolaurat): Sigma-Aldrich cat.no. P9416
- VectaMount AQ Aqueous Mounting Medium: Vector Laboratories, cat.no. H-5501
- Xylazine (Rampun) 2%: Bayer Vital

2.1.5 Buffers

Anesthetic solution

- 0.9 % NaCl (wt/vol)
- 125 µL Ketamine
- 25 µL Xylazine

BSA Blocking solution (for immunohistochemistry)

- 5 % BSA (wt/vol)
- 0.3 % Triton X-100 (vol/vol)

➔ In 1x PBS

Bradford solution

- 0.01 % Serva Blue (vol/vol)
- 8.5 % Phosphoric acid (vol/vol)
- 4.75 % Ethanol (vol/vol)

➔ in H_2O

Buffer A

- Sucrose 0,32 M
- HEPES 5 mM

➔ In aqua deionized

➔ Before use add 1 tablet protease-inhibitor to 50 mL buffer A

Buffer B

- Sucrose 0.32 M
- Tris-HCl 5 mM

➔ In aqua deionized

Buffer C

- Sucrose 0.32 M
- Tris 12 mM
- Triton 1 % (vol/vol)

➔ In aqua deionized

Crude synaptosomal fraction buffer

- Hepes 4 mM
- Sucrose 320 mM

➔ In aqua deionized

Dilution buffer (for western blot probes)

- 0.32 M Sucrose
- 4 mM HEPES

➔ In aqua deionized at pH 7.4

Running buffer 10x

- 13.3 g Tris
- 144 g glycin
- 10 g SDS

➔ add aqua deionized until 1 L volume

Loading buffer 4x

- 200mM Tris HCl, pH 6.8
- 200mM DTT
- 4 % SDS (wt/vol)

- 4mM EDTA
- 40 % glycerol (vol/vol)
- 0.002 % Bromphenol blue (10 mg / mL) (vol/vol)

PBS 10x (pH 7.4)

- 80g NaCl (pH 7.4)
- 2g KCl
- 14.4g Na2HPO4x2H2O
- 2.4g KH2PO4

➔ add HCl until pH is 7.4

➔ add aqua deionized until 1 L volume

Skim milk powder blocking solution 5 % (for western blot)

- 5 % milk powder (wt/vol)

➔ In 100 mL 0.1% TBST (vol/vol)

Skim milk powder blocking solution 3 % (for western blot)

- 3 % milk powder

➔ In 100 mL 0.1 % TBST (vol/vol)

Sucrose 0.85 M

- Sucrose 0.85 M
- Tris-HCl 5 mM

➔ In aqua deionized

Sucrose 1 M

- Sucrose 1 M
- Tris-HCl 5 mM

➔ In aqua deionized

Sucrose 1.2 M

- Sucrose 1.2 M
- Tris HCl 5 mM

➔ In aqua deionized

TBS 10x (pH 7.6)

- 61 g Tris
- 90 g NaCl

➔ add HCl until pH is 7.6

➔ add aqua deionized until 1 L volume

TBST 0.1 %

- 1 L 1x TBS
- 1 mL TWEEN 20

Trans-Blot buffer

- 200 mL TransBlot®Turbo™ 5x Transfer Puffer
- 200 mL Ethanol
- 600 mL H2O

2.1.6 Stock Solutions

Ammonium persulfate 10 % (wt/vol)

- 1 g APS

➔ add 10 mL with aqua deionized

➔ Store at 4 °C

SDS 10 % (wt/vol)

- 10 g Sodium dodecyl sulfate
- 100 mL aqua deionized

Tris 1 M pH 6.8

Tris 1.5 M pH 8.8

2.1.7 Recipes

Anesthetic solution (250 µL)

- 175 µL NaCl 0.9 % (wt/vol)
- 62.5 µL Ketamine
- 12.5 µL Xylazine

➔ Enough for one animal

Western blot 10% running gel (5mL)

- 1.9 mL H_2O
- 1.7 mL Acrylamide/Bis Solution
- 1.3 mL Tris 1.5 M pH 8.8
- 0.05 mL SDS 10%
- 0.05 mL Ammonium pesruslafe 10%
- 0.002 mL TEMED

Western blot stack gel (= 1 mL)

- 0.68 mL H_2O
- 0.17 mL Acrylamide/Bis Solution
- 0.13 mL Tris 1 M pH 6.8
- 0.01 mL SDS10%
- 0.01 mL Ammonium pesruslafe 10%
- 0.001 mL TEMED

2.1.8 Consumable supplies

- 24-well plates: Falcon, cat.no. 353047
- 6-well plates: Falcon, cat.no. 353046
- 96-well plates: Cellstar, Greiner, cat.no. 655180
- Dry ice: Pharmacy of the Clinic of the University of Ulm
- Glass coverslips: Karl Hecht GmbH, Sondheim, cat.no. 1001/13
- Glass Pasteur Pipette: Brand, cat.no. 747715
- Leica Microsystems Immersion Oil: Thermo-Fischer, cat.no. 11513859
- Liquid nitrogen: Linde Gas
- Long plastic pipettes: Greiner Bio-One
- Nail polish: Cosnova
- Nitrocellulose blotting membrane 0.2 µm: GE Healthcare, Life Sciences, cat.no.

10600004

- PageRuler Plus Prestained Protein Ladder, 10 to 250 kDa: Thermo-Fischer, cat.no.26619
- Peel-A-Way Embedding Mold (Square - S22): Polysciences, inc, cat.no. 18646A-1
- Pipette tips 10 µL, 200 µL, 1000 µL: Eppendorf
- Razor blades: Aesculap AG
- Reaction tubes 0.5 mL: Eppendorf, cat.no. 0030121023
- Reaction tubes 1.5 mL: Eppendorf, cat.no. 0030120086
- Reaction tubes 2 mL: Eppendorf, cat.no. 0030120094
- Reaction tubes 15 mL: Sarstedt, cat.no. 62.554.001
- Reaction tubes 50 mL: Sarstedt, cat.no. 62.547.254
- Trans-Blot Turbo Midi-size Nitrocellulose: Bio-Rad, cat.no. BR20150917
- Trans-Blot Turbo Midi-size Transfer Stacks: Bio-Rad, cat.no. BR20150705
- Ultra-Clear™ Tubes: Beckman Coulter, cat.no. 344057
- Whatman filter papers: Schleicher & Schuell

2.1.9 Labware

- Autoclave: Systec, Germany, Münster
- Avanti J-25: Beckman Coulter, Germany, Krefeld
- Axio Imager. Z1: Zeiss, Germany, Oberkochen
- Biofuge Fresco: Kendro Laboratory, Germany, Hanau
- Centrifuge 5430 R: Eppendorf, Germany, Hamburg
- Centrifuge 5804 R Eppendorf, Germany, Hamburg
- CM3050 S (Cryostat): Leica, Germany, Nussloch
- Dissection Tools: Fine science tools, Germany, Heidelberg
- Eppendorf Thermomixer comfort: Eppendorf AG, Germany, Hamburg
- Freezer (-20°C): Liebherr, Germany, Biberach
- Freezer (-80°C): Thermo Scientific, USA, Waltham
- Glass plates: Biorad, Germany, Munich

- Horizontal shaker: Sigma-Aldrich, USA, St. Louis
- Ice cube maker: ZIEGRA Eismaschinen, Germany, Isernhagen
- Incubator: Binder, Germany, Tuttlingen
- Magnetic stirrer: IKA, Germany, Staufen
- MicroChemi 4.2: DNR Bio Imaging Systems, Israel, Neve Yamin
- Optima Max-E Ultracentrifuge: Beckman Coulter, Germany, Krefeld
- Perfusor (and connected tubes): Ismatec, USA, Berrington
- Pipetboy: Hirschmann, Germany, Eberstadt
- Pipettes: Eppendorf, Germany, Hamburg
- PowerPac Basic Power Supply: Biorad, USA, Hercules
- Potter S: B. Braun Biotech international, Germany, Melsungen
- Refrigerator (4°C): Liebherr, Germany, Biberach
- Rotator: Stuart-Equipment, cat.no. SB2
- TCS SPE II (Confocal Microscope): Leica, Germany, Nussloch
- Tissue Grinder: Nippon Genetics Europe, Germany, Düren
- Trans-Blot® Turbo™ Transfer System: Biorad, USA, Hercules
- Vortexer: Heraeus, Germany, Hanau

2.1.10 Software

- AxioVision 4.8: Carl Zeiss, Germany, Oberkochen
- Excel 2010: Microsoft, USA, Redmond
- GelCapture 2.0
- ImageJ 1.46r: NIH, USA, Bethesda,
- Leica LAS X interface
- PowerPoint 2010: Microsoft, USA, Redmond
- Word 2010: Microsoft, USA, Redmond

2.2 Methods

2.2.1 Protein Biochemistry

2.2.1.1 Killing of the mice

The mice were anesthetized by flooding a chamber with CO_2 until the toe pinch test showed to be negative. Then they were decapitated with a guillotine. I was supported in the procedure by Dr. Michael Schoen, my supervisor for the project.

2.2.1.2 Brain region preparation

Taking the skin of the head of the skull was done by cutting it in a median line from occipital to rostral on the dorsal side of the head with a pair of scissors. The skull was opened from the foramen magnum to the nose, also in a median line on the dorsal side of the skull with a very small pair of scissors. Since this is where the fissura longitudinalis cerebri is located it is a good location to split the skull because it is less likely to damage the brain tissue when cutting. Incisions are then made orthogonally to the median one. This creates little rectangles of skull bone that can easily be chipped away with a pair of tweezers. Optionally, an incision can be made between the orbitae by simply cutting the bone with a pair of scissors. When that bone is then chipped away with a pair of tweezers it is easier to extract the olfactory bulb without damaging it. When the entire head including the brain is now tipped backwards, the brain will want to fall out of the base of the skull but will not be able to because it is still attached via the brain nerves, which now become visible. Hence, they should be severed with a small pair of scissors. At last, the brain can be extracted from the skull with a very small spoon. It can then be frozen with liquid nitrogen and subsequently either frozen away at -80 °C or kept for further usage. I was supported in the procedure by Anna Nusser, a fellow M.D. student at the laboratory.

2.2.1.3 Crude synaptosomal fractions

Centrifuge homogenates at 1000 g for 10 minutes. Extract the supernatant and centrifuge it at 10000 g for 15 minutes. Discard the supernatant and resuspend the pellet in crude synaptosomal fraction buffer. The volume of the buffer depends on the amount of pellet. I was supported in the procedure by Dr. Christopher Heise.

2.2.1.4 Bradford-Assay

In a 24-well plate, fill the wells with 1mL Bradford solution each. Add to the top 6 wells: 0, 2, 4, 6, 8, 10 µL BSA 1 mg / mL, these are the reference solutions. Add the tissue homogenates to the other wells, 1 µL per well and assess the protein concentration by comparing to the reference solutions. Dilute the homogenates accordingly in order to reach a protein concentration of 1.5 µg / mL, with half of the probe being running buffer. I was supported in the procedure by Dr. Christopher Heise.

2.2.1.3 Western blot

Stacking gels and running gels were freshly prepared before every experiment. The protein ladder and the samples were loaded on the gels and an electric current of 120 V was applied. As soon as the samples passed the stacking gel, the electric current was increased to 210 V until the desired separation of proteins was reached. After the electrophoresis, the gel was transferred on to a Trans-Blot® Turbo™ Midi-size Nitrocellulose Membrane. This membrane was then placed on to a Trans-Blot® Turbo™ Midi-size Transfer Stack, inside of a container and another transfer stack was placed on top of it, creating a sandwich. The sandwich was moistened by Trans-Blot buffer. Transferring the proteins from the gel on to the membrane was performed in a Trans-Blot® Turbo™ Transfer System using the mixed molecular weight program (25 V for 7 min) twice. The nitrocellulose was then blocked for 1 hour at 4 °C in

skim milk powder blocking solution 5 %. Then the nitrocellulose was incubated in the primary AB in skim milk powder blocking solution 3 % over night at 4 °C. The secondary AB incubation was performed with skim milk powder blocking solution 3 % for 1 hour at RT. Pierce ECL western blotting substrate was dripped on to the membrane and then pictures were taken in the MicroChemi 4.2 with GelCapture 2.0. I was supported in the procedure by Dr. Christopher Heise.

2.2.1.4 PSD-Fractioning

The tissue probes were mixed with 10 mL buffer A per g tissue and then homogenized with the Potter S at 900 rpm. The homogenate was transferred into a new falcon and a probe was taken = Ho. The homogenate was centrifuged in the Biofuge Fresco at 1000 g and 4 °C for 10 min. The supernatant was transferred into a new falcon and a sample was taken from it = S1. The pellet was dissolved in buffer A (10 mL buffer A per g tissue) and centrifuged in the Biofuge Fresco at 1000 g and 4 °C for 10 minutes. This supernatant was then added to the previous one and a probe was taken from the pellet = P1 (either dissolved in the leftover supernatant that cannot be extracted or in very little buffer A). S1 was centrifuged in the Avanti J-25 at 12000g and 4 °C for 20 minutes. A probe was taken from the supernatant = S2. The rest of the supernatant was discarded and the pellet was dissolved in buffer A, 10 mL per g tissue (original weight was taken). This was centrifuged in the Avanti J-25 at 12000 g and 4 °C for 20 minutes. The supernatant was discarded and a probe was taken from the pellet = P2. The rest of the pellet was dissolved in buffer B, 1.5 mL buffer B per g tissue. The sucrose gradient was made from sucrose solutions with 0.85 M; 1 M; 1.2 M. 1 mL of each was put into an ultra-centrifuge-tube, beginning with the lowest molarity and always adding the next higher one under the previous one with a pasteur pipette. Buffer B – pellet mixture was put on top of the sucrose gradient. This was then centrifuged in the Optima Max-E Ultracentrifuge at 40000 rpm and 4 °C for 2 hours. The fractions were collected: top = Myl; second layer = LM (polysomes, golgi apparatus, smooth endoplasmic reticulum); third layer = Syn; bottom = Mit. Mix Syn probe with the same volume (1:1) of buffer C. The probes were inverted on the rotator at 4 °C for 10 minutes. The Syn probe was centrifuged in the Optima Max-E Ultracentrifuge at 25000 rpm and 4 °C for 1

hour. A probe of the supernatant was taken = S3 (as much as necessary) and the rest of the supernatant was discarded. The pellet was mixed with 100 µL ddH2O and a probe was taken = P3 (as much as necessary). I was supported in the procedure by Anna Nusser.

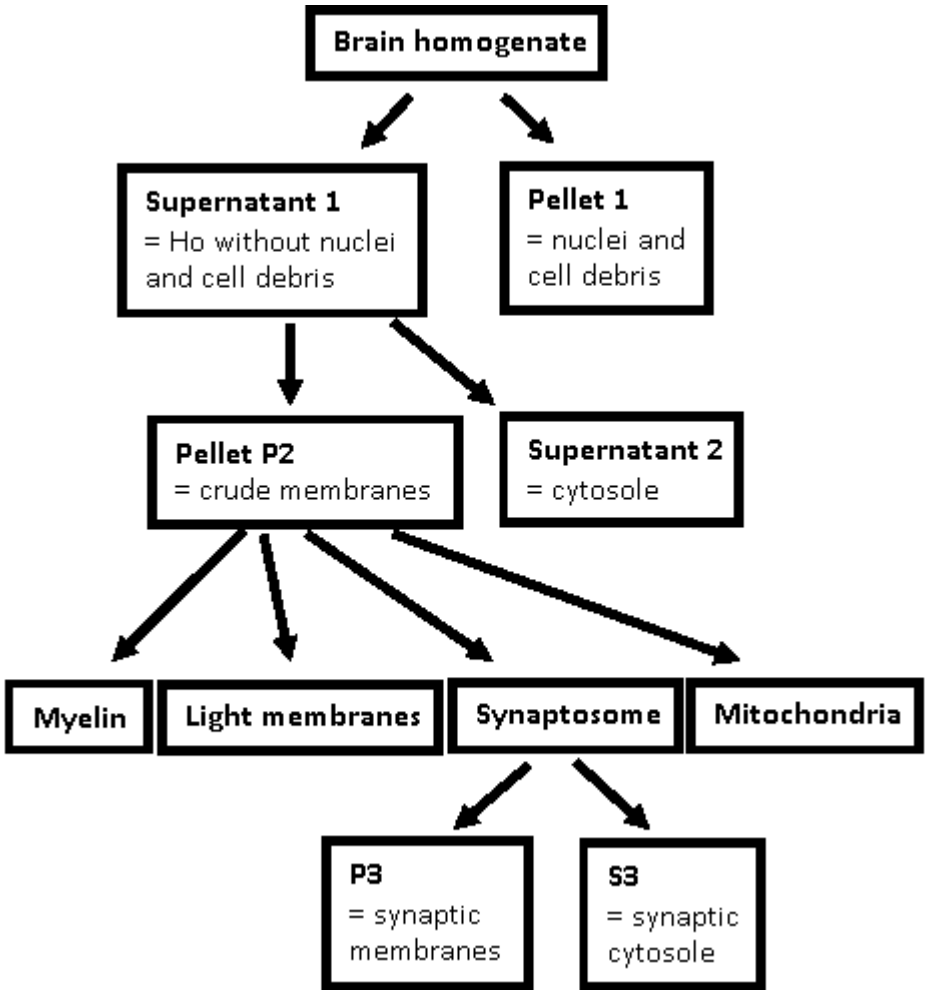

Figure 2: Schema of steps for PSD fractioning

2.2.2 Immunohistochemistry

2.2.2.1 Mouse Perfusion

Day 1 – Perfusion: I prepared 250 µL anesthetic solution per animal and injected it intraperitoneal. I performed the toe pinch test to make sure the animal was deeply anaesthetized. I opened up the abdominal and thoracic cavities. Then I made a small incision into the right atrium with scissors and inserted the cannula into the apex of the heart, which is part of the left. I ran the pump with 1 x PBS, ~25 mL at 5 mL/min. The pump was stopped and then run again with 4 % (wt/vol) PFA in 1 x PBS (pH 7.4), 45-50 mL. Then I extracted the brain and stored it in a small falcon in 4 % PFA (pH 7.4) over night. Day 2 – sucrose: I transferred the brain into a small falcon with 30 % (wt/vol) sucrose in 1x PBS until it did not float towards the surface anymore which took a night. Day 3 – freezing: Once the brain sank to the bottom of the falcon, I gently dried it on filter paper. I set a Peel-A-Way on a block of dry ice and filled it with a little Tissue-Tek. Then I laid the brain in the Tissue-Tek as soon as the bottom part of it turned hard but the top was still soft. Then I filled the Peel-A-Way up with Tissue-Tek all the way and waited until it turned completely hard. Lastly, I stored it in the -80°C freezer. I was supported in the procedure my Mrs. Renate Zienecker, a laboratory technician.

2.2.2.2 Cryostat slicing

I removed as much of the Tissue-Tek around the brain as possible with razor. Then I cut it in the Leica CM3050 S, 40 µm thick. After that I transferred the slices into a 24-well plate, max. 4 slices per well in 1x PBS. I was supported in the procedure by Mrs. Renate Zienecker.

2.2.2.3 Staining

All following steps were performed on a shaker. I block the slices in BSA Blocking solution for 2 h at RT. Then I incubated with the primary AB in BSA Blocking solution for 48 h – 72 h at -4 °C. I washed with 1 x PBS, 3 times for 30 min each. From here on the slices had to be kept in the dark as much as possible. I incubated with the secondary AB in BSA Blocking solution for at least 2 h at RT. I washed with DAPI 1:10000 in 1 x PBS, 1 time for 30 min. Then I washed with 1 x PBS, 2 times for 30 min each. I dropped 1x $PBS^{-/-}$ on a cover slide (1 large drop per slice) and moved the slice into the drop. I removed as much of the 1 x PBS as possible with a 100 µL pipette and let the slice dry, only until it just lost its liquid glossiness. I put large drops of Vecta Mount on the object slide where the slices were going to lay and slowly laid the cover glass on the object slide. Then I let it dry for at least half a day at 4 °C. I was supported in the procedure by Mrs. Ursula Picka-Hartlaub, a laboratory technician.

2.2.2.4 Microscopy

These images for the following figures were all made with a confocal microscope and the computer software Leica LAS X interface. I was supported in the procedure by Dr. Michael Schön.

Figure 1, GS3 (GFP-SHANK3) & WT:

Laser 405; Laserpower 11,5; Filter 430 - 480; Digital Gain 900

Laser 488; Laserpower 50; Filter 500 - 565; Digital Gain 900

Figure 2, GS3 & WT:

Laser 405; Laserpower 35; Filter 430 nm - 480 nm; Digital Gain 900

Laser 488; Laserpower 65; Filter 500 nm - 565 nm; Digital Gain 900

Figures 5-7 for bassoon, GS3 & WT:

Laser 405; Laserpower 4,46; Filter 430 nm - 480 nm; Digital Gain 900

Laser 488; Laserpower 45,6; Filter 500 nm - 565 nm; Digital Gain 900

Laser 561; Laserpower 33; Filter 567 nm - 630 nm; Digital Gain 900

Figures 5-7 for SHANK2, wild type & transgenic animal:

Laser 405; Laserpower 27,1; Filter 433 nm - 486 nm; Digital Gain 900

Laser 488; Laserpower 35; Filter 500 nm - 553 nm; Digital Gain 900

Laser 561; Laserpower 14; Filter 569 nm - 622 nm; Digital Gain 900

Figure 63x striatum:

Laser 405; Laserpower 4,46; Filter 430 nm - 480 nm; Digital Gain 900

Laser 488; Laserpower 45,6; Filter 500 nm - 565 nm; Digital Gain 900

Laser 561; Laserpower 33; Filter 567 nm - 630 nm; Digital Gain 900

Figures 6 & 7

The images for these figures were all made with the fluorescence microscope ‘Axio Imager. Z1’ and the computer software AxioVision 4.8. All images within each one figure were made with the same exposure time.

3. Results

Two complementary methods (namely: immunohistochemistry and western blotting) were used to analyze whether, indeed, GFP-SHANK3 (GS3) expression takes place at all in our transgenic mice and - if so - in which brain regions and subcellular compartments it is localized to. Also, synaptic GS3 expression was characterized more closely by evaluating colocalization of GS3 (a mostly postsynaptically localized protein) with the postsynaptic marker SHANK2 and the presynaptic marker bassoon.

3.1 Imaging of GFP-SHANK3 mouse brains using Immunohistochemistry

The imaging was done at three levels of observation. (1) An overview of an entire coronal brain slice containing the hippocampus/striatum, (2) an overview of each the hippocampus/striatum at 5x magnification and (3) at 63x magnification to analyze hippocampal sub regions with synaptic resolution. For reference to the neuroanatomical descriptions of the figures the Allen brain atlas was used (Allen institute for brain science 2011).

3.1.1 General overviews of brain slices (figures 3 & 4)

The images show, that there is a stark difference between the green signal (488nm; GFP-GS3) of the transgenic mouse and that of the wild type: the wildtype is devoid of GFP-GS3 stain. Also, the fluorescence is not distributed evenly over the entirety of the slice but is strongly more intense in (1) the cortex, (2) the hippocampus and (3) the striatum.

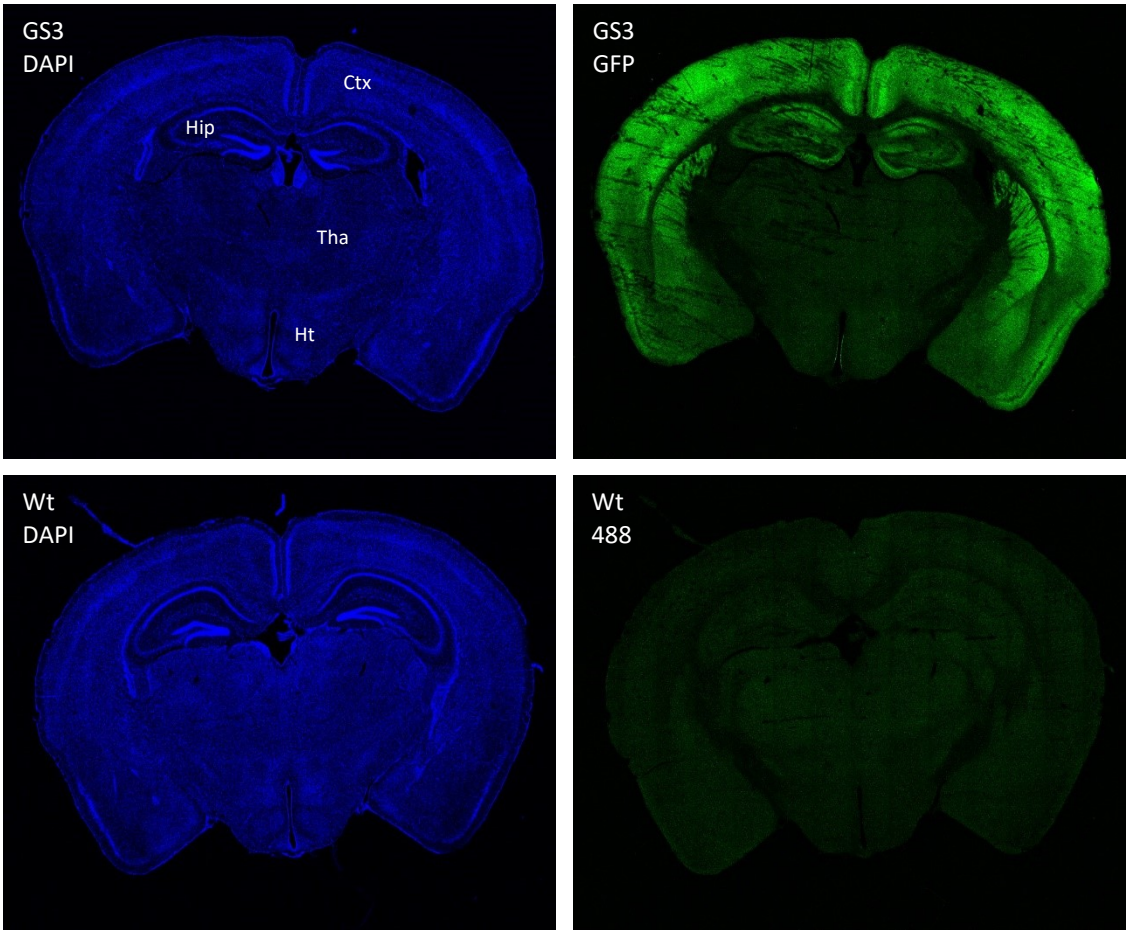

Figure 3: GFP-SHANK3 expression takes place in the hippocampi and cortices of *GFP-Shank3* transgenic mice. The analyzed regions are coronal brain slices corresponding to the allen brain atlas image 75. Representative images of one WT and one GS3 transgenic mouse are shown. **1** = DAPI stain of a transgenic animal; **2** = GFP-SHANK3 signal of the same transgenic animal; **3** = DAPI stain of a wildtype animal; **4** = no signal in the 488 nm wavelength channel of the same wild type animal. **GS3** = GFP-Shank3 (transgenic animal); **Wt** = wildtype; **Ctx** = cortex; **Hip** = hippocampus; **Tha** = thalamus; **Ht** = hypothalamus

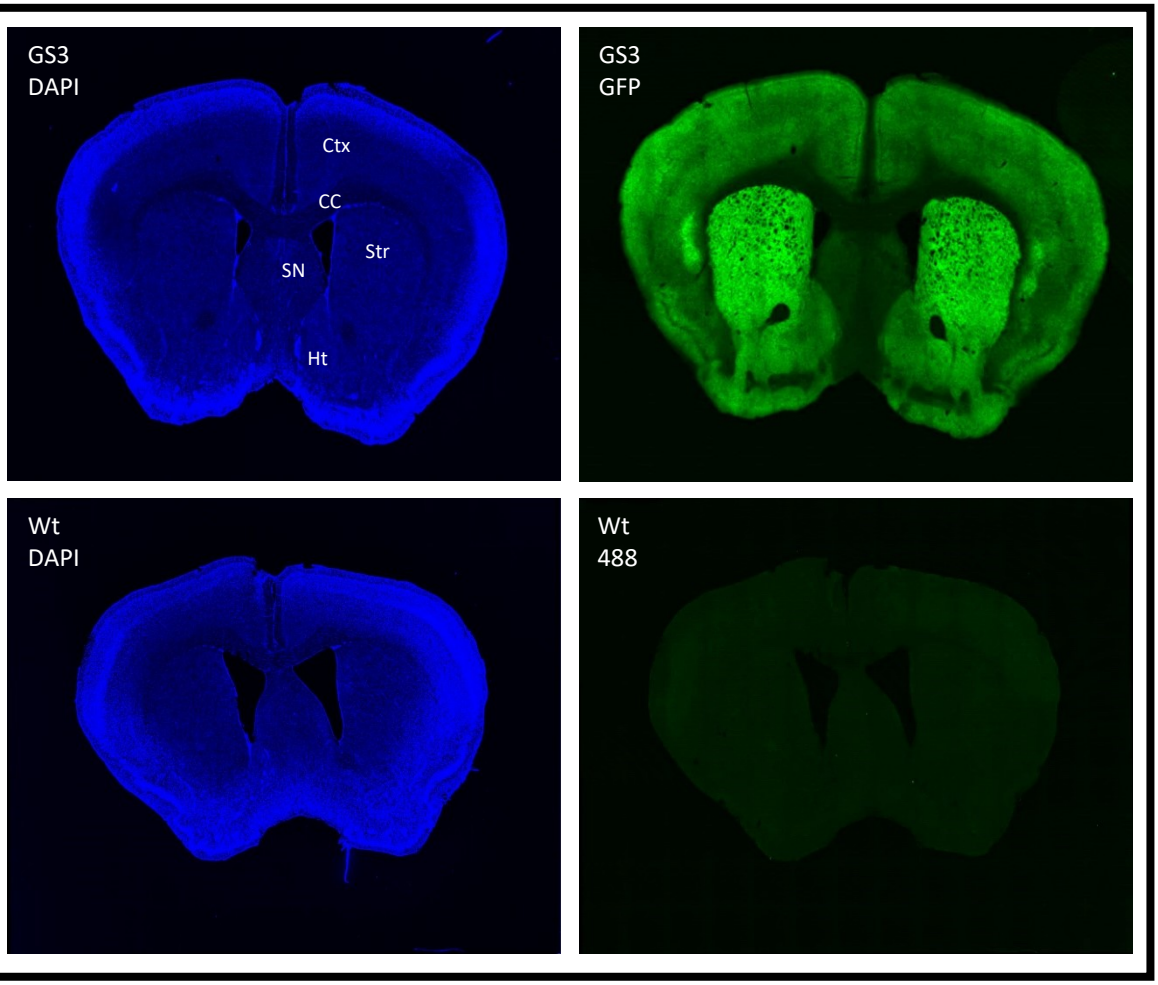

Figure 4: GFP-SHANK3 expression takes place in the striata and cortices of *GFP-Shank3* transgenic mice. The analyzed regions are coronal brain slices corresponding to the allen brain atlas image 50. Representative images of one WT and one GS3 transgenic mouse are shown. **1** = DAPI stain of a transgenic animal; **2** = GFP-SHANK3 signal of the same transgenic animal; **3** = DAPI stain of a wildtype animal; **4** = no signal in the 488 nm wavelength channel of the same wild type animal. **GS3** = GFP-Shank3 (transgenic animal); **Wt** = wildtype; **Ctx** = cortex; **Cc** = corpus callosum; **Str** = striatum; **SN** = septal nucleus; **Ht** = hypothalamus

3.1.2 Hippocampal & striatal overviews (figures 5 & 6)

The main goal of the hippocampal and striatal overviews is to see whether the green GFP signal is expressed in specific regions of the hippocampus and the striatum, or if it is just being expressed everywhere without subregion-specificity. **Image 6** shows that there is further specificity not only to the hippocampus itself, but to specific sub-regions of the hippocampus. The fluorescence signal is - as expected for a synaptic protein like SHANK3 - especially weak in all layers with somata (e.g. granular layer in the dentate gyrus) but enriched in layers with synapses (e.g. polymorph layer in the dentate gyrus).

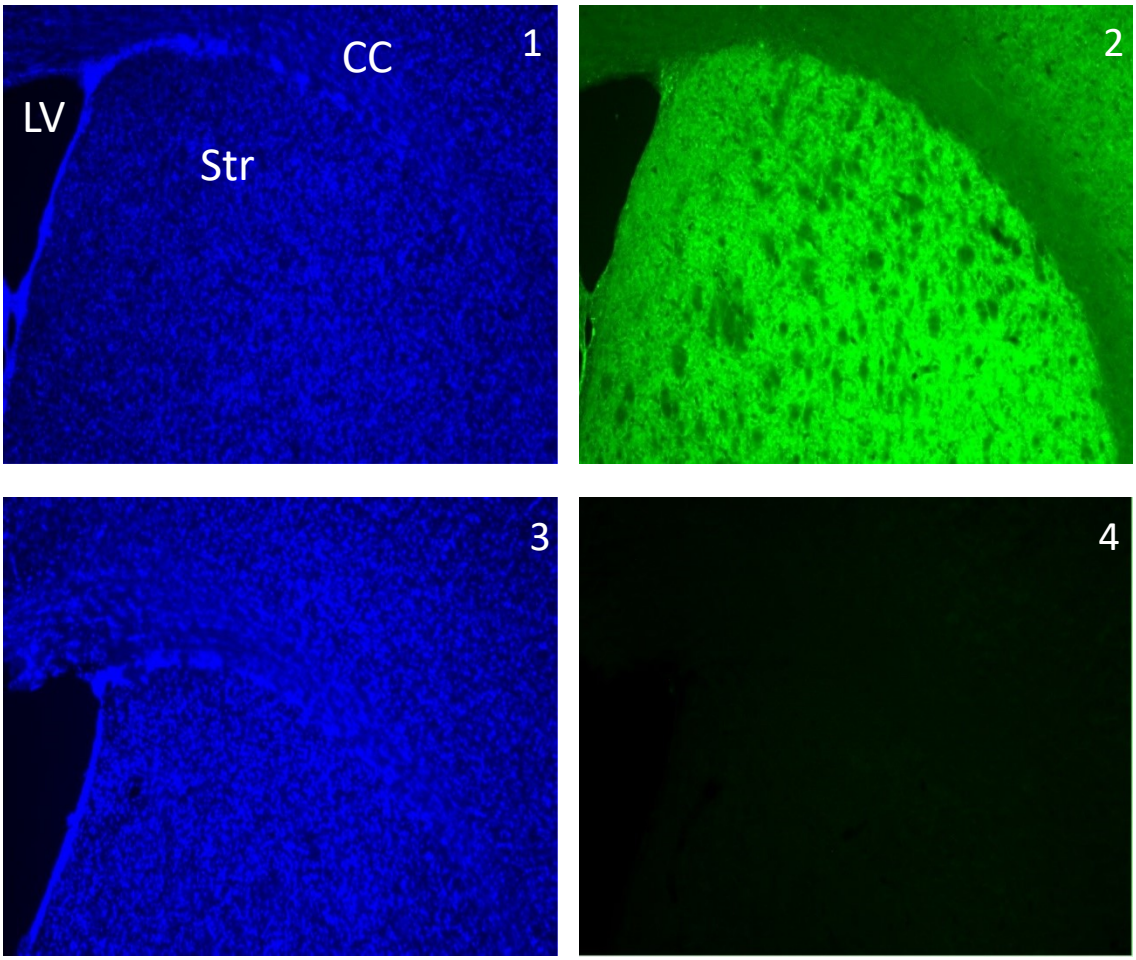

Figure 5: GFP-SHANK3 expression takes place in the striata of *GFP-Shank3* transgenic mice. Representative images of one WT and one GS3 transgenic mouse are shown. The analyzed region is the striatum. **1** = DAPI stain of a transgenic animal; **2** = GFP-SHANK3 signal of the same transgenic animal; **3** = DAPI stain of a wildtype animal; **4** = no signal in the 488 nm wavelength channel of the same wild type animal. **GS3** = GFP-SHANK3 (transgenic mouse); **Wt** = wildtype; **LV** = lateral ventricle; **CC** = corpus callosum; **Str** = striatum.

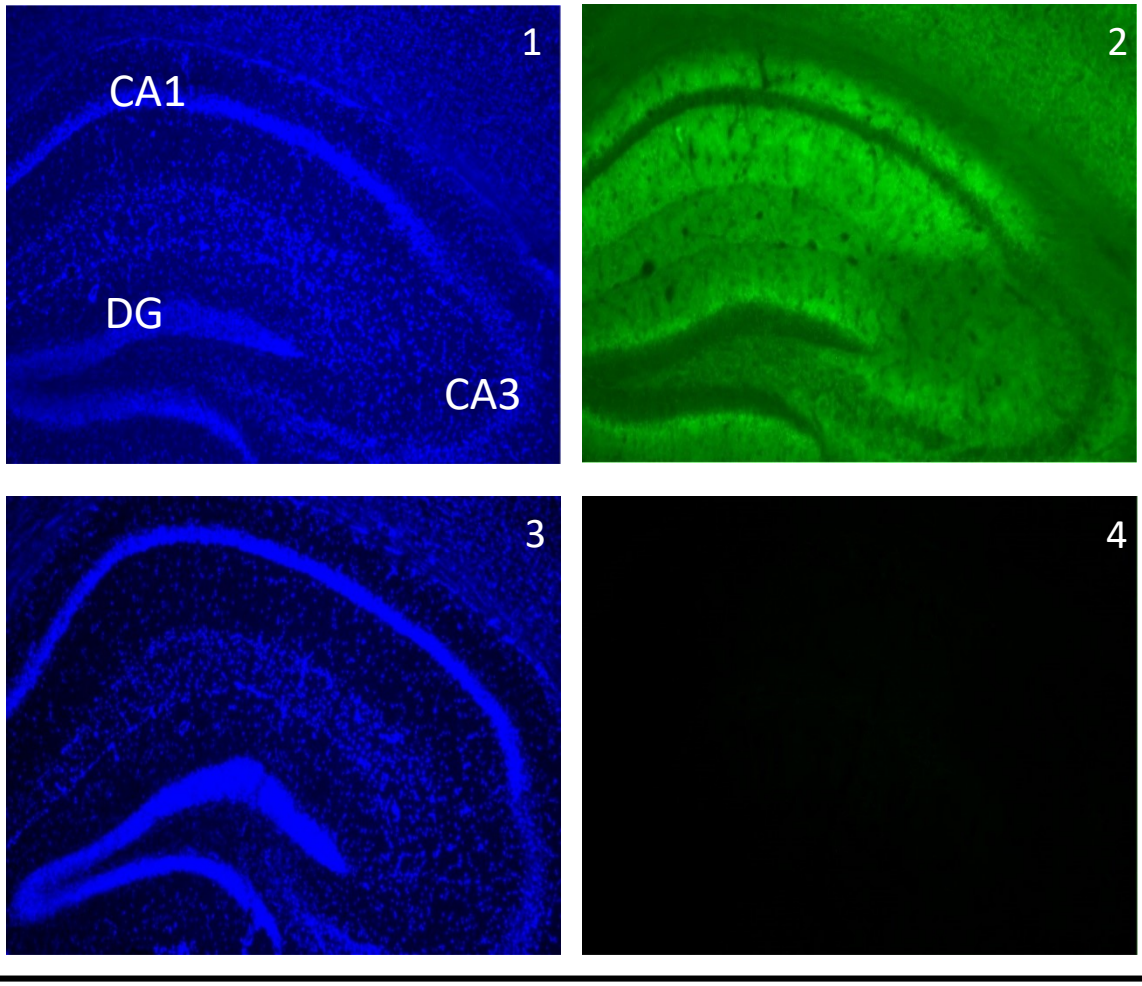

Figure 6: GFP-SHANK3 expression takes place in the hippocampi of *GFP-Shank3* transgenic mice. Representative images of one WT and one GS3 transgenic mouse are shown. The analyzed region is the hippocampus. **1** = DAPI stain of a transgenic animal; **2** = GFP-SHANK3 signal of the same transgenic animal; **3** = DAPI stain of a wildtype animal; **4** = no signal in the 488 nm wavelength channel of the same wild type animal. **DG** = dentate gyrus; **CA3** = CA3 region; **CA1** = CA1 region

3.1.3 Detailed images of hippocampus and striatum at 63x magnification (figures 7 - 10)

The main purpose of the detailed **images 7-10** is an attempt to show the colocalization of the (transgenic) GFP-SHANK3 (GS3) with pre- and postsynaptic markers. This is what we would expected since (endogenouse) SHANK3 is synaptically localized. Bassoon was used as a presynaptic marker and SHANK2 was used as a postsynaptic marker.

3.1.3.1 Detailed images of the dentate gyrus (Figure 7)

Figure 7 shows a close-up of the hippocampal dentate gyrus and confirms the impression from **figure 6**, that the green fluorescent signal is located extremely sparsely around the somata of the granular cell region and much more abundantly around the cell processes of the polymorph and molecular layer. **Row 2** shows the colocalization of GFP with the postsynaptic marker Bassoon in the molecular and polymorph layers. An enlargement of the polymorph layer shows this colocalization in more detail. **Row 1** shows a wild type, also stained with Bassoon but lacking the GFP signal and thus the colocalization. **Row 4** shows the colocalization of GFP with the presynaptic marker SHANK2, also in the molecular and polymorph layers. Again, an enlargement of the polymorph layer shows this colocalization in more detail. **Row 3** shows a wild type, also stained with SHANK2, but lacking the GFP signal and thus the colocalization.

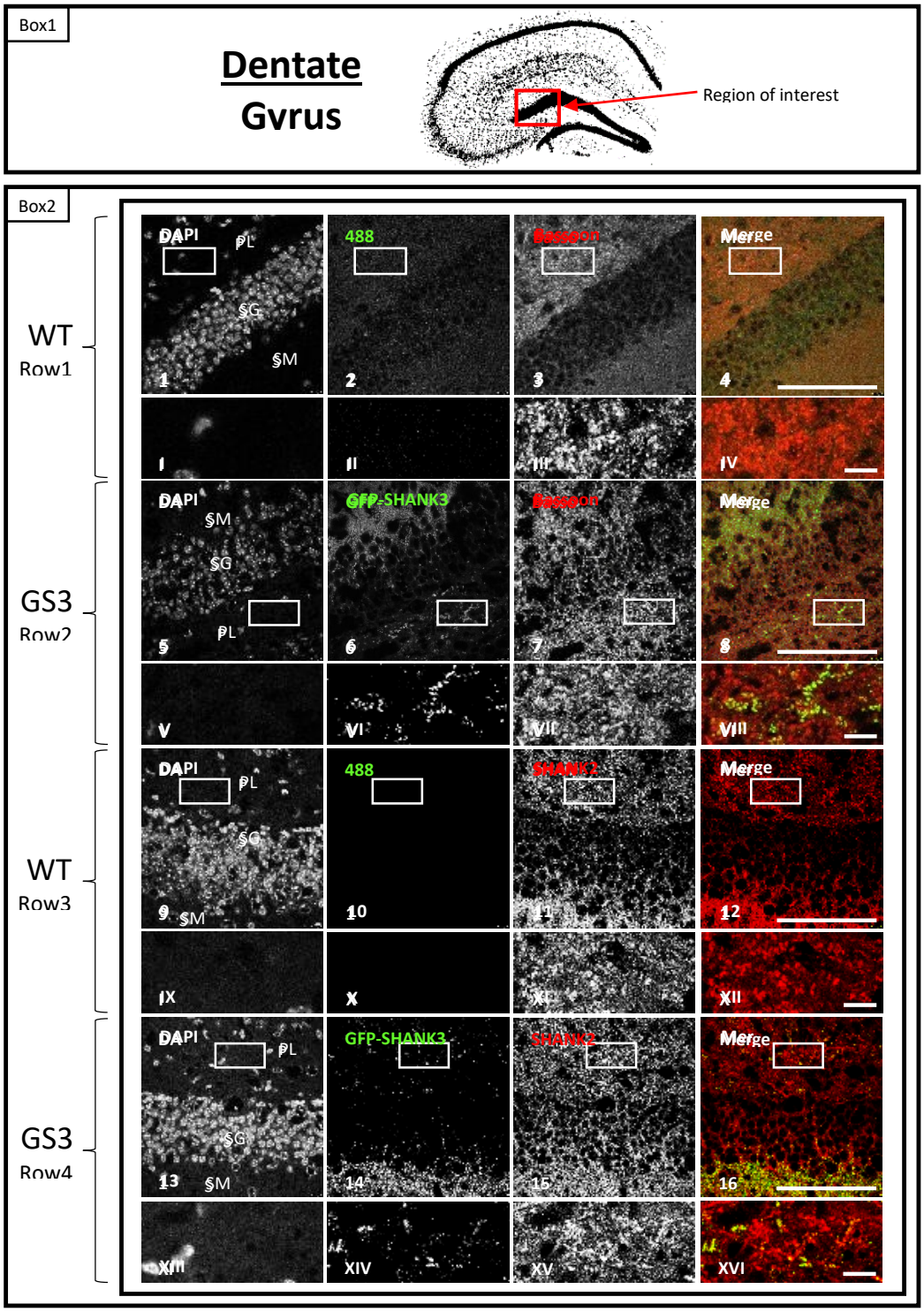

Figure 7: Colocalization of GFP-Shank3 with the presynaptic marker bassoon and with the postsynaptic marker Shank2. The analyzed region is the hippocampal dentate gyrus. **Box 1** contains a schematic overview of the hippocampus with the enlarged region of interest marked by a square. It encompasses the polymorph layer = **PL**, the granular layer = **SG** and the molecular layer = **SM**. **Box 2** contains representative immunofluorescence stainings of coronal mouse brain slices. The larger images are 63x magnifications, while the small images are enlargements of the large ones. **Row 1** (Images 1 – 4 & I – IV) shows a wild type animal (WT = wild type) stained with antibodies directed against Bassoon. **Row 2** (Images 5 – 8 & V – VIII) shows a transgenic animal (GS3 = GFP-Shank3) stained with fluorescent antibodies directed against Bassoon. **Row 3** (Images 9 – 12 & IX – XII) shows a wild type animal stained with fluorescent antibodies directed against Shank2. **Row 4** (Images 13 – 16 & XIII – XVI) shows a transgenic animal stained with fluorescent antibodies directed against Shank2. **The large squares** (arab numbers) show the enlarged region from box 1 (scale bar = 100 µm). **The bottom rectangles** (roman numbers) show further enlargements, marked in the large squares by white rectangles (scale bar = 10 µm). In the merge, GFP-Shank3 is shown in green and Bassoon/Shank2 is shown in red.

3.1.3.2 Detailed images of the CA3 region (Figure 8)

In **figure 8**, the pyramidal layer, containing the cell somata, shows nearly no fluorescent GFP signals. Almost all of the fluorescence of the GFP is found in the stratum lucidum and less in the stratum oriens. **Row 2** shows the colocalization of GFP with the postsynaptic marker Bassoon in the stratum oriens and stratum lucidum. An enlargement of the stratum lucidum shows this colocalization in more detail. **Row 1** shows a wild type, also stained with Bassoon but lacking the GFP signal and thus the colocalization. **Row 4** shows the colocalization of GFP with the presynaptic marker SHANK2, also in the stratum oriens and stratum lucidum. Again, an enlargement of the stratum lucidum shows this colocalization in more detail. **Row 3** shows a wild type, also stained with SHANK2, but lacking the GFP signal and thus the colocalization.

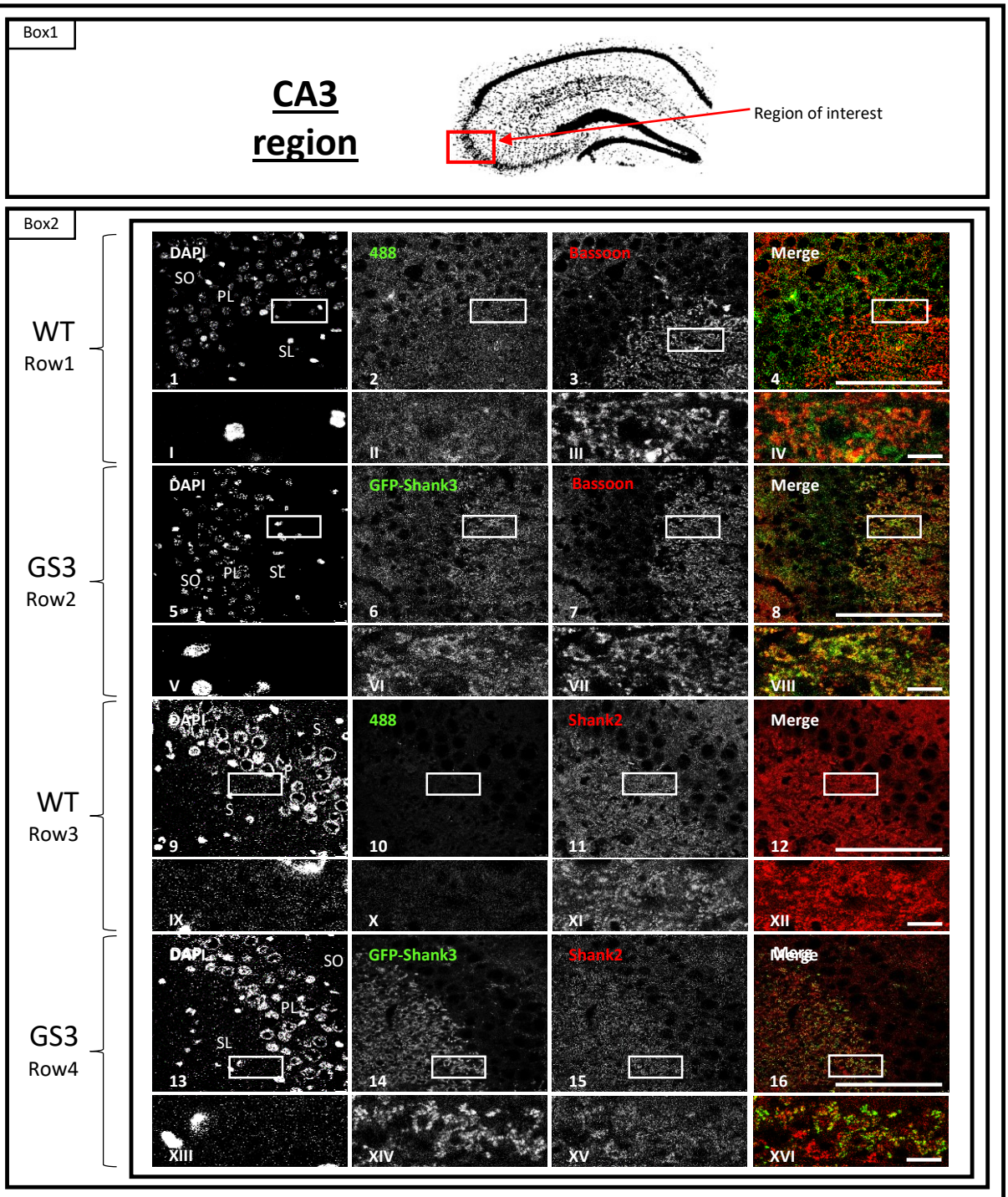

Figure 8: Colocalization of GFP-Shank3 with the presynaptic marker bassoon and with the postsynaptic marker Shank2. The analyzed region is the hippocampal CA3 region. **Box 1** contains a schematic overview of the hippocampus with the enlarged region of interest marked by a square. It encompasses the stratum oriens = **SO**, pyramidal layer = **PL** and the stratum lucidum = **SL**. **Box 2** contains representative immunofluorescence stainings of coronal mouse brain slices. The larger images are 63x magnifications, while the small images are further enlargements of the large ones. **Row 1** (Images 1 – 4 & I – IV) shows a wild type animal (WT = wild type) stained with antibodies directed against Bassoon. **Row 2** (Images 5 – 8 & V – VIII) shows a transgenic animal (GS3 = GFP-Shank3) stained with antibodies directed against Bassoon. **Row 3** (Images 9 – 12 & IX – XII) shows a wild type animal stained with antibodies directed against Shank2. **Row 4** (Images 13 – 16 & XIII – XVI) shows a transgenic animal stained with antibodies directed against Shank2. . **The large squares** (arab numbers) show the enlarged region from box 1 (scale bar = 100 µm). **The bottom rectangles** (roman numbers) show further enlargements, marked in the large squares by white rectangles (scale bar = 10 µm). In the merge, GFP-Shank3 is shown in green and Bassoon/Shank2 is shown in red.

3.1.3.3 Detailed images of the CA1 region (Figure 9)

Figure 9 shows a close-up of the hippocampal CA1 region. The green fluorescent signal is again located extremely sparsely around the somata of the pyramidal layer and much more abundantly around the cell processes of the stratum oriens and the stratum radiatum. **Row 2** shows the colocalization of GFP with the postsynaptic marker Bassoon in the stratum oriens and stratum radiatum. An enlargement of the stratum radiatum shows this colocalization in more detail. **Row 1** shows a wild type, also stained with Bassoon but lacking the GFP signal and thus the colocalization. **Row 4** shows the colocalization of GFP with the presynaptic marker SHANK2, also in the stratum oriens and stratum radiatum. Again, an enlargement of the stratum radiatum shows this colocalization in more detail. **Row 3** shows a wild type, also stained with SHANK2, but lacking the GFP signal and thus the colocalization.

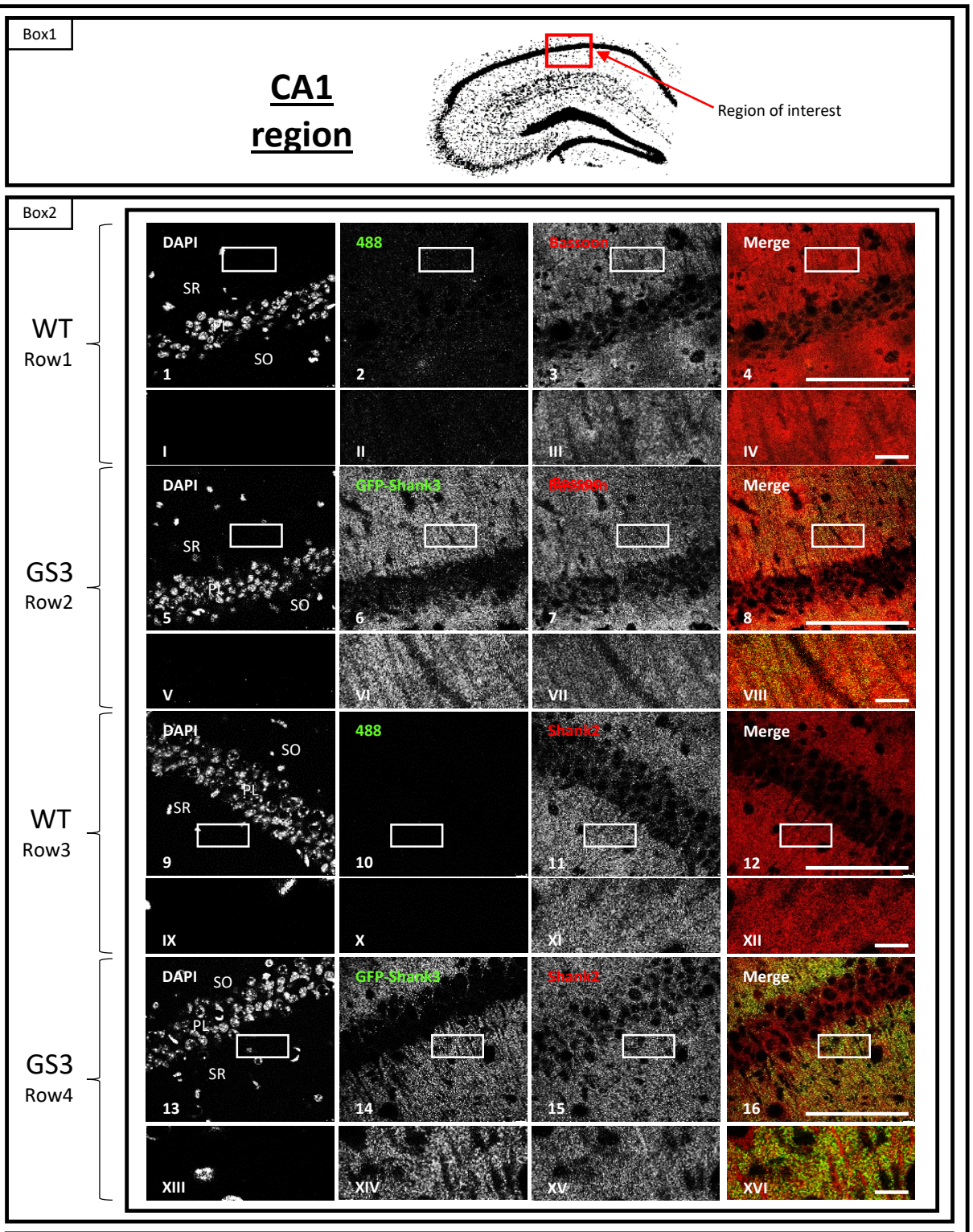

Figure 9: Colocalization of GFP-Shank3 with the presynaptic marker bassoon and with the postsynaptic marker Shank2. The analyzed region is the hippocampal CA1 region. **Box 1** contains a schematic overview of the hippocampus with the enlarged region of interest marked by a square. It encompasses the stratum oriens = **SO**, pyramidal layer = **PL** and the stratum radiatum = **SR**. **Box 2** contains representative immunofluorescence stainings of coronal mouse brain slices. The larger images are 63x magnifications, while the small images are further enlargements of the large ones. **Row 1** (Images 1 – 4 & I – IV) shows a wild type animal (WT = wild type) stained with antibodies directed against Bassoon. **Row 2** (Images 5 – 8 & V – VIII) shows a transgenic animal (GS3 = GFP-Shank3) stained with antibodies directed against Bassoon. **Row 3** (Images 9 – 12 & IX – XII) shows a wild type animal stained with antibodies directed against Shank2. **Row 4** (Images 13 – 16 & XIII – XVI) shows a transgenic animal stained with antibodies directed against Shank2. **The large squares** (arab numbers) show the enlarged region from box 1 (scale bar = 100 µm). **The bottom rectangles** (roman numbers) show further enlargements, marked in the large squares by white rectangles (scale bar = 10 µm). In the merge, GFP-Shank3 is shown in green and Bassoon/Shank2 is shown in red.

3.1.3.4 Detailed images of the striatum (Figure 10)

Figure 10 shows a close-up of the dorsomedial striatum. The green GFP signal is distributed evenly throughout the striatum and shows colocalization with the presynaptic marker bassoon.

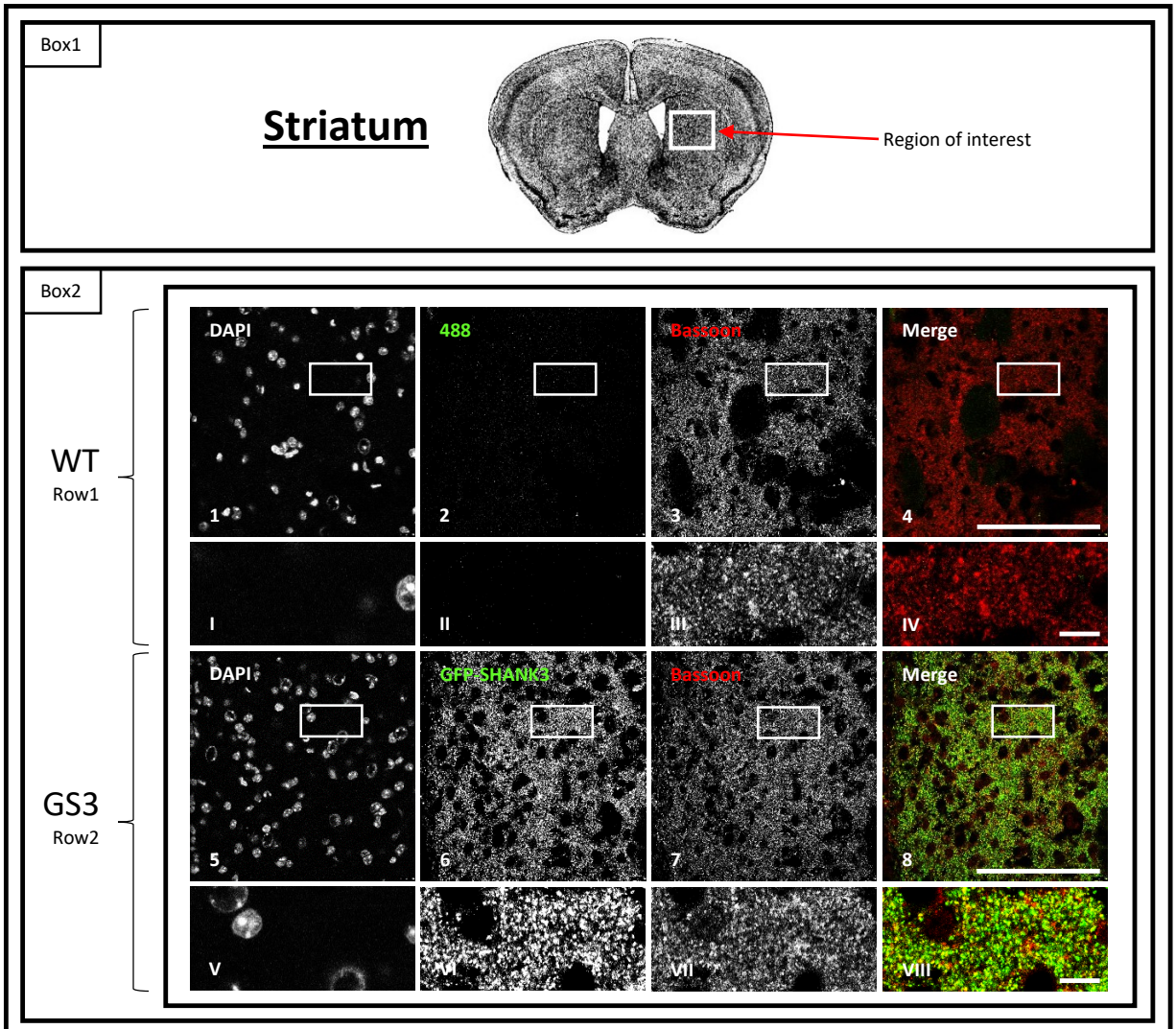

Figure 10: Colocalization of GFP-SHANK3 with the presynaptic marker bassoon. The analyzed region is the striatum. **Box 1** contains a schematic overview of a coronal brain slice with the enlarged region of interest marked by a square. **Box 2** contains representative immunofluorescence stainings of coronal mouse brain slices. The larger images are 63x magnifications, while the small images are further enlargements of the large ones. **Row 1** (Images 1 – 4 & I – IV) shows a wild type animal (WT = wild type) stained with antibodies directed against bassoon. **Row 2** (Images 5 – 8 & V – VIII) shows a transgenic animal (GS3 = GFP-Skank3) stained with antibodies directed against bassoon. **The large squares** (arab numbers) show the enlarged region from box 1 (scale bar = 100 µm). **The bottom rectangles** (roman numbers) show further enlargements, marked in the large squares by white rectangles (scale bar = 10 µm). In the merge, GFP-SHANK3 is shown in green and bassoon/SHANK2 is shown in red.

3.2 Protein biochemistry of GFP-SHANK3 mouse brains

The western blots were done for different purposes: (1) A comparison between the crude synaptosomal fractions of different brain regions of transgenic animals and wild types. (2) A comparison between the subcellular fractions of the entire brain of transgenic animals and wild types. Here, the aim was to analyze whether exogenous GS3 localizes to synaptic fractions as endogenous SHANK3 does.

3.2.1 Crude synaptosomal fractions of hippocampus and cortex (figures 11 & 12)

The goals were first (1) to generally show that there is a GFP signal endogenously expressed by the transgenic animals and not by the wild types. Second, (2) that its molecular weight is in accordance with a fusion protein of GFP and SHANK3.

Figures 11 & **12** both show that there is a clear difference in the expression of GFP in the transgenic animal versus the wild type animal, namely that it is virtually not present in the wild type. Furthermore, the pattern of the expression is very similar to that of the isolated GFP-SHANK3 protein used as a control. The control GFP-SHANK3 protein was recombinant rat GFP-SHANK3 isolated from cos7-cells and kindly provided by Ms. Carolina Urrutia-Ruiz. It is also observable that the SHANK3 signal is noticeably stronger in the transgenic animals than it is in the wild types.

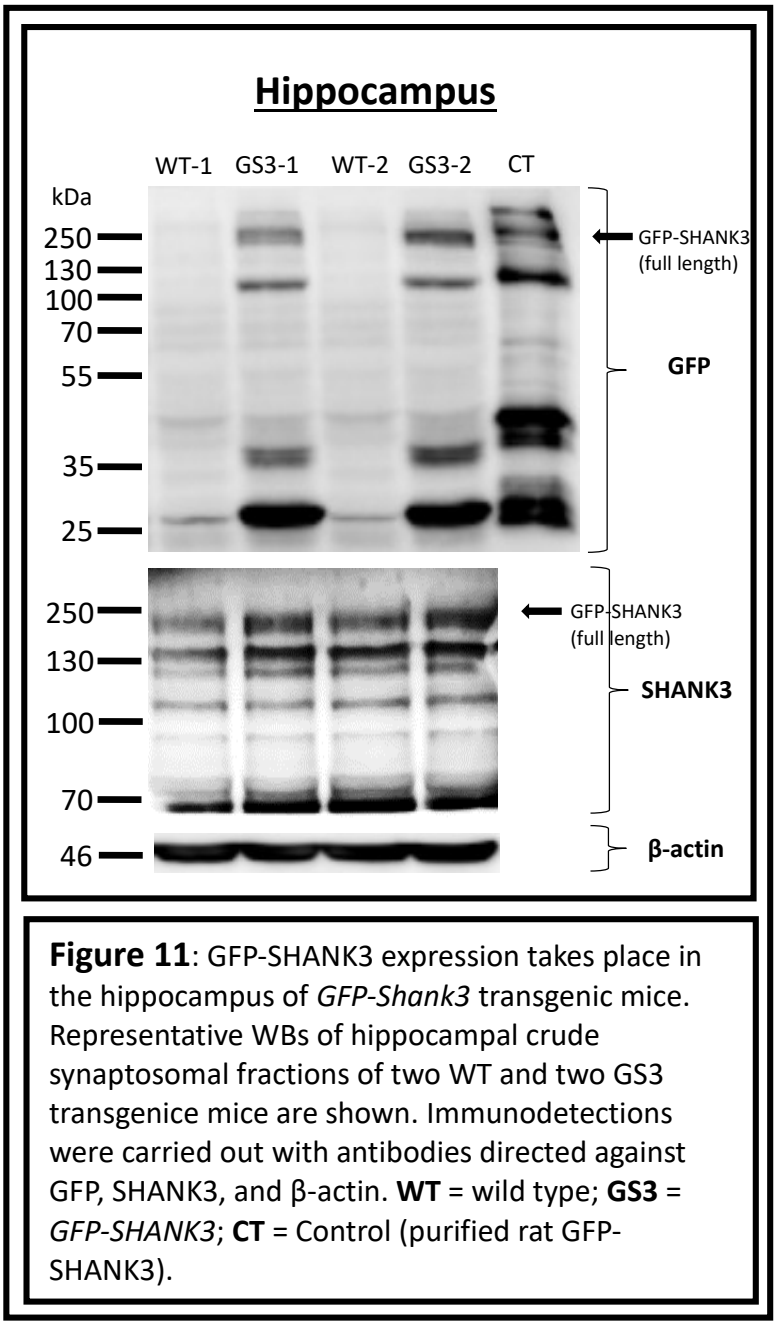

Figure 11: GFP-SHANK3 expression takes place in the hippocampus of *GFP-Shank3* transgenic mice. Representative WBs of hippocampal crude synaptosomal fractions of two WT and two GS3 transgenice mice are shown. Immunodetections were carried out with antibodies directed against GFP, SHANK3, and β-actin. **WT** = wild type; **GS3** = *GFP-SHANK3*; **CT** = Control (purified rat GFP-SHANK3).

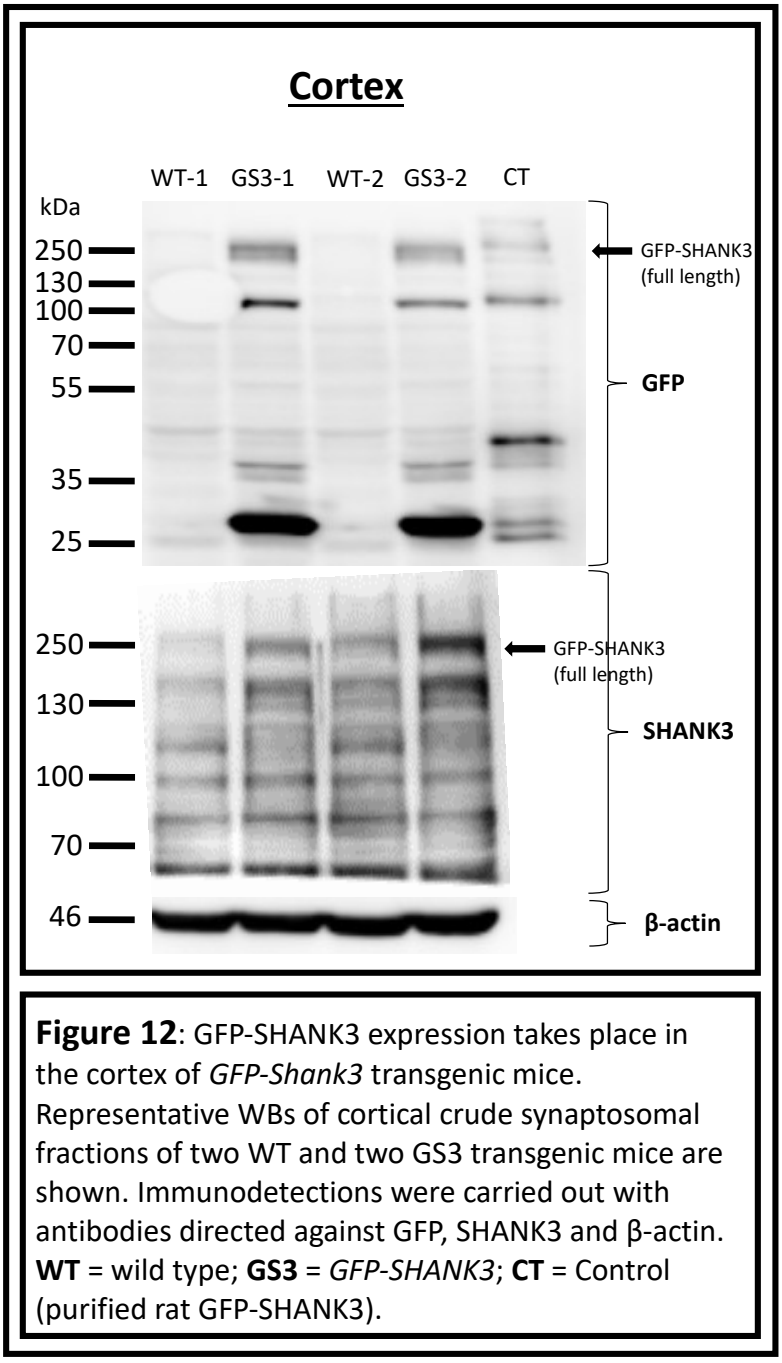

Figure 12: GFP-SHANK3 expression takes place in the cortex of *GFP-Shank3* transgenic mice. Representative WBs of cortical crude synaptosomal fractions of two WT and two GS3 transgenic mice are shown. Immunodetections were carried out with antibodies directed against GFP, SHANK3 and β-actin. **WT** = wild type; **GS3** = *GFP-SHANK3*; **CT** = Control (purified rat GFP-SHANK3).

3.2.2 Crude synaptosomal fractions of the brain regions (figure 13)

The specific goal of these western blots is to compare the expression of the GFP-SHANK3 protein in the different regions of the brain to each other.

Figure 13 shows that for both the GFP and the SHANK3 signals there is a difference between the transgenic and the wild type animal for some brain regions, but not for others. The regions for which there seems to be a difference appear to be (1) the thalamus, (2) the hippocampus, (3) the striatum, and (4) the cortex. The regions in which there appears to be no difference between the transgenic animal and the wild type are (1) the cerebellum and (2) the brain stem.

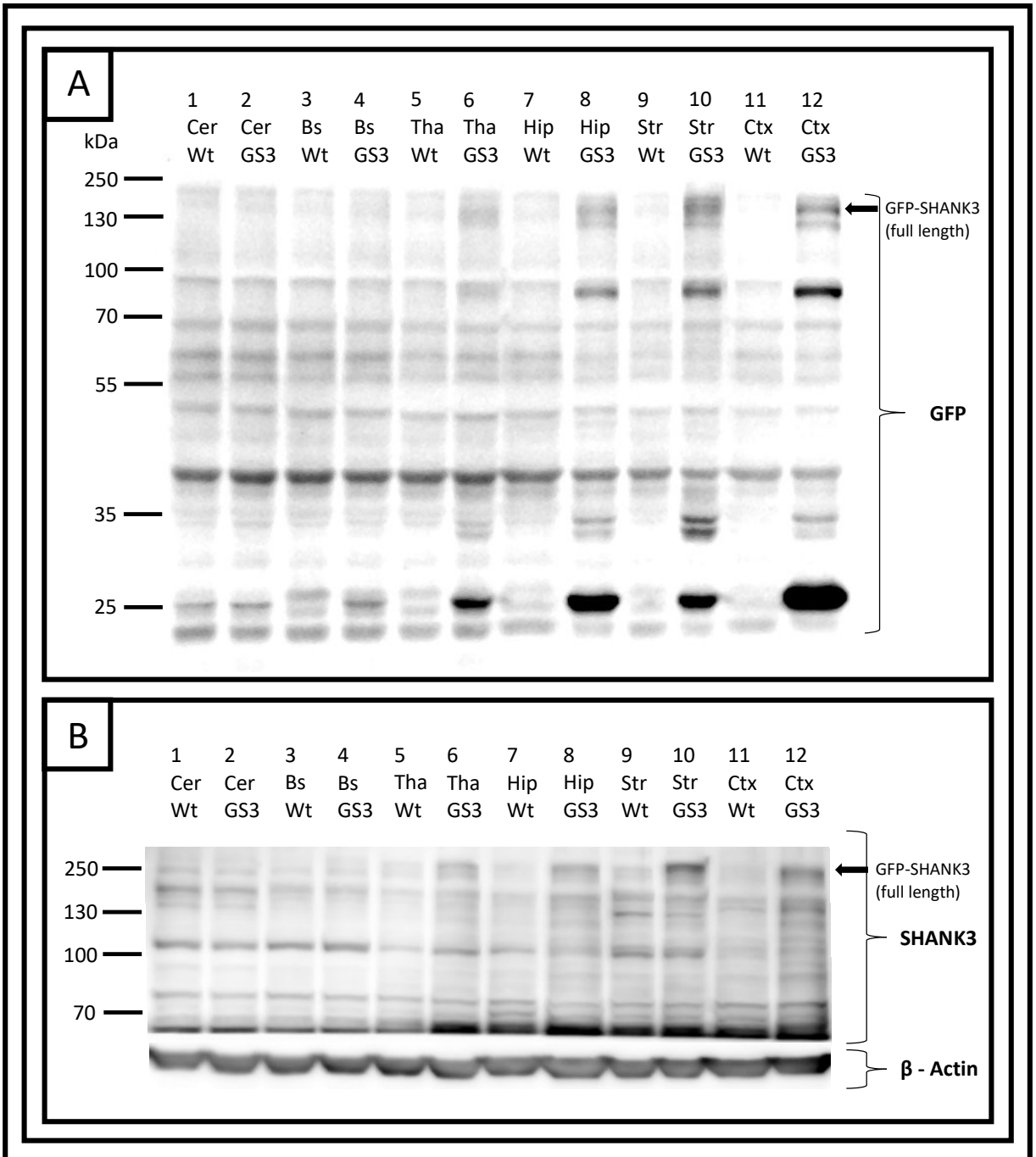

Figure 13: GFP-SHANK3 expression takes place differently in different brain regions of *GFP-Shank3* transgenic mice. Representative western blots of crude synaptosomal fractions of one WT and one GS3 transgenic animal are shown. Immunodetections were carried out with antibodies directed against GFP **(A)**, SHANK3 **(B)** and β-actin **(B)**. The β-actin blot is representative for the SHANK3 blot as well as for the GFP blot since the same probes were used for all three of them. **Wt** = wildtype; **GS3** = GFP-SHANK3 (transgenic animal); **Cer** = cerebellum; **Bs** = brainstem; **Tha** = thalamus; **Hip** = hippocampus; **Str** = striatum; **Ctx** = cortex.

3.2.3 Subcellular compartments

Here, we wanted to see two things: (1) If the signals are enriched in synaptic/membraneous compartments, as would be expected for a synaptically located GFP-SHANK3 protein. (2) If the endogenous GFP-SHANK3 signal behaves as other postsynaptic proteins do.

3.2.3.1 SHANK3 staining on a WT & GFP staining on a transgenic animal (Figure 14)

The most prominent information that **figure 14** reveals is that the GS3 expressions differ in different compartments of the cell. Looking at it more closely, one can extract four relevant pieces of information from the figure: (1) The signal in Ho, S1, P1 & P2 seems to be similarly strong. The signal in S2, however, looks weaker, even though the β-actin band is the strongest out of the first five. (2) In a next step one can see that of the fractions Myl, LM and Syn, the GFP signal seems to be strongest in the Syn fraction. (3) Between the S3 and the P3 compartments, the GFP signal is unquestionably stronger in the P3 compartment. (4) Lastly, when comparing **figure 14B** to **14A**, it is evident that the distribution of the transgenic GFP signal matches that of the wild type SHANK3 signal.

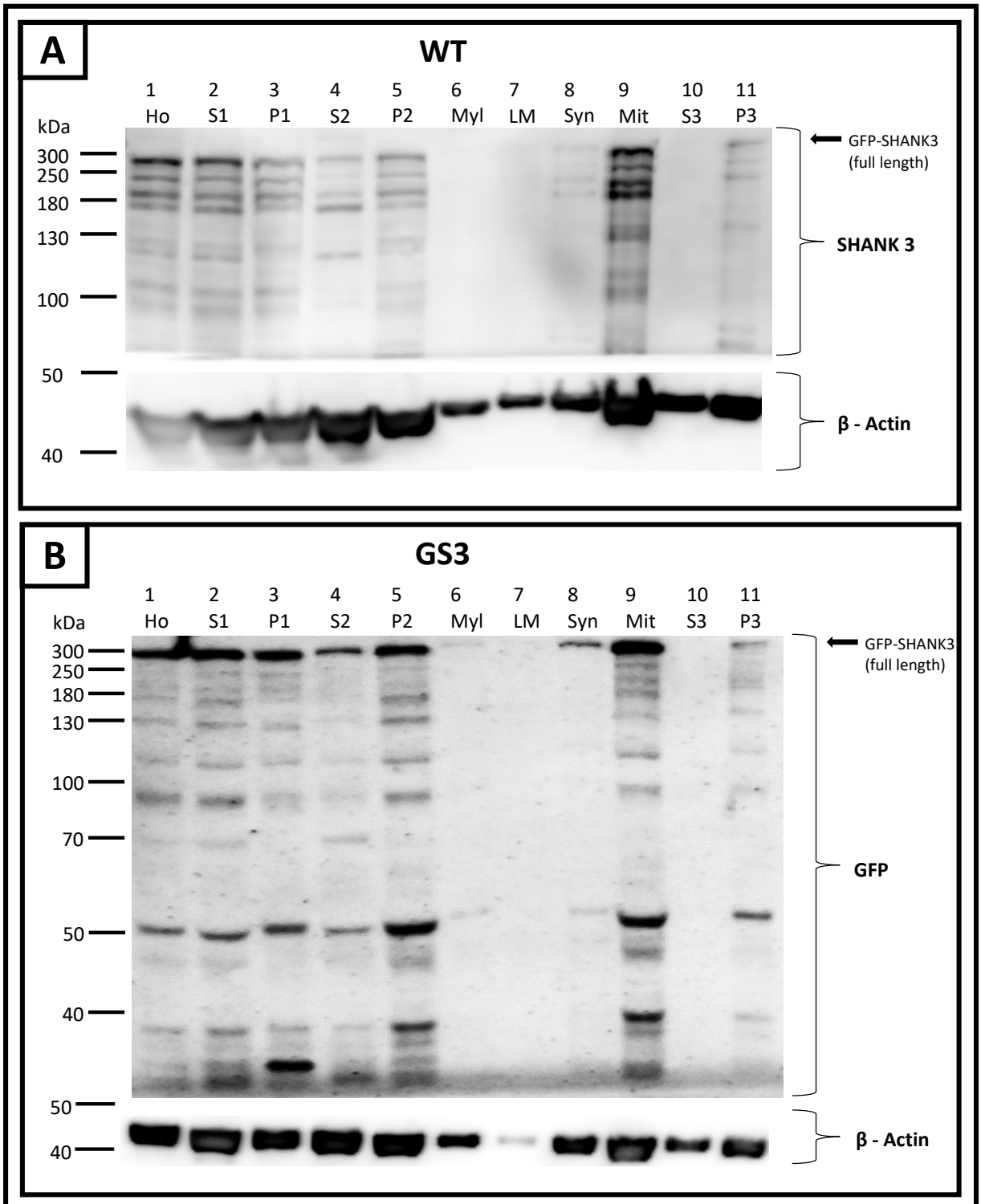

Figure 14: Endogenous SHANK3 and transgenic GFP-SHANK3 display a similar subcellular localization. Representative WBs of subcellular compartments of one WT **(A)** and one GS3 transgenic **(B)** mouse are shown. Immunodetections were carried out with antibodies directed against Shank3 **(A)**, GFP **(B)** and β-actin. The β-actin blot in box **(B)** was taken from a different western blot made with the same probes under the same conditions. **Ho** = homogenate; **S1** = homogenate without nuclei & cell debris (S for supernatant); **P1** = nuclei & cell debris (P for pellet); **S2** = cytosole; **P2** = crude membranes; **Myl** = myelin; **LM** = light membranes; **Syn** = synaptosome; **Mit** = mitochondria; **S3** = synaptosomal cytosole; **P3** = synaptosomal membranes.

3.2.3.2 SHANK3 staining on a transgenic animal & PSD-95 staining on a WT (Figure 15)

Figure 15 is complementary to **figure 14**. Here, there are three notable things to be observed: (1) Firstly, the transgenic SHANK3 signal of **figure 15A** has the same pattern among the subcellular compartments as the transgenic GFP signal of **figure 14B**. (2) Secondly, the pattern of the transgenic SHANK3 signal of **figure 15A** has a comparable pattern among the subcellular compartments as the wild type PSD-95 signal from **figure 15B**. (3) And lastly the pattern of the signal of the wild type PSD-95 signal of **figure 15B** has the same pattern among the subcellular compartments as the transgenic GFP signal from **figure 14B**.

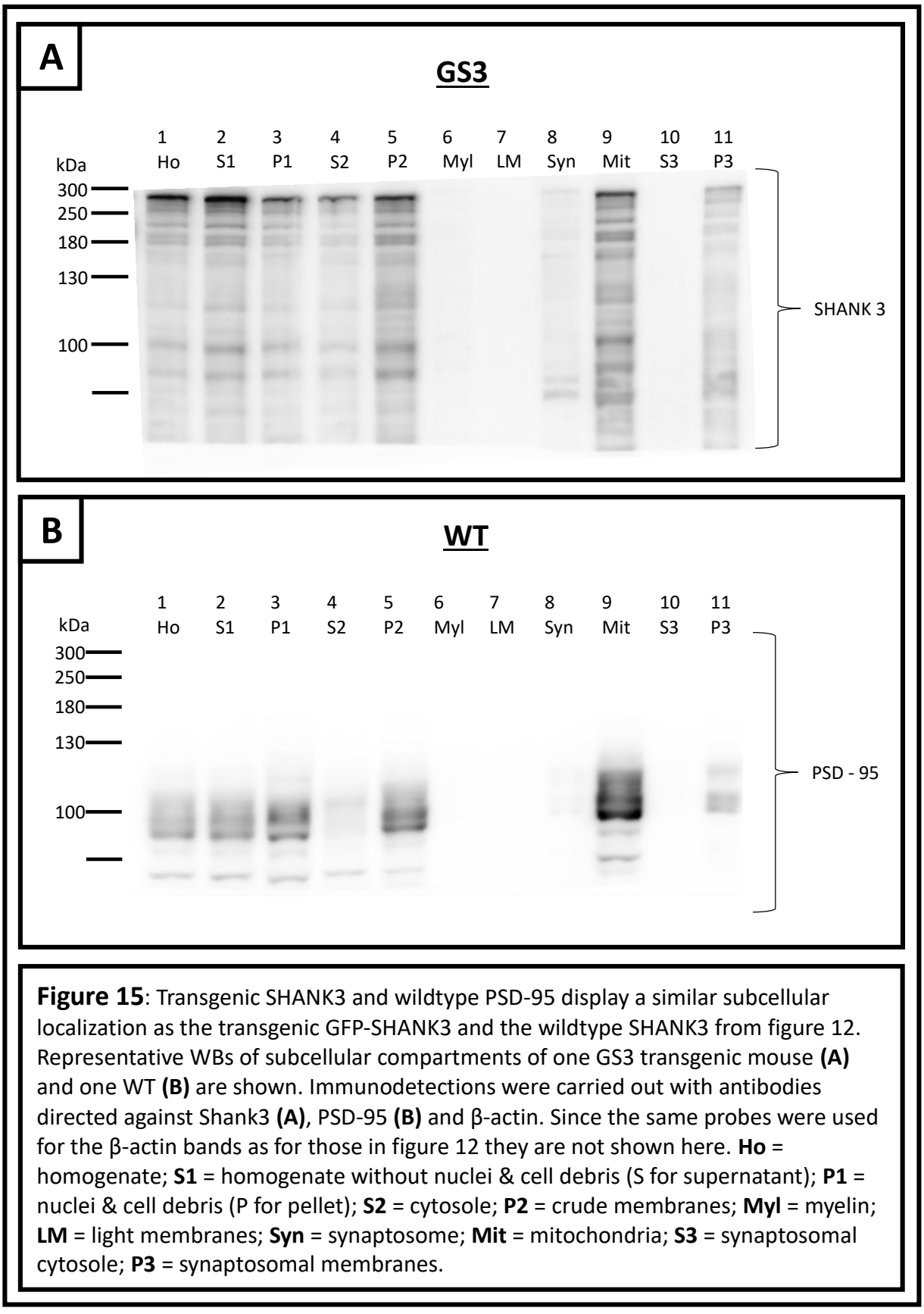

Figure 15: Transgenic SHANK3 and wildtype PSD-95 display a similar subcellular localization as the transgenic GFP-SHANK3 and the wildtype SHANK3 from figure 12. Representative WBs of subcellular compartments of one GS3 transgenic mouse **(A)** and one WT **(B)** are shown. Immunodetections were carried out with antibodies directed against Shank3 **(A)**, PSD-95 **(B)** and β-actin. Since the same probes were used for the β-actin bands as for those in figure 12 they are not shown here. **Ho** = homogenate; **S1** = homogenate without nuclei & cell debris (S for supernatant); **P1** = nuclei & cell debris (P for pellet); **S2** = cytosole; **P2** = crude membranes; **Myl** = myelin; **LM** = light membranes; **Syn** = synaptosome; **Mit** = mitochondria; **S3** = synaptosomal cytosole; **P3** = synaptosomal membranes.

4. Discussion

4.1 General findings

The results of this thesis yield the following findings: (1) The transgenic mouse expresses GFP, (2) the GFP is linked to SHANK3 in form of a GFP-SHANK3 fusion protein, (3) the GFP-SHANK3 protein is specific to the forebrain and (4) it is synaptically located.

4.2 General expression of the GFP-SHANK3 fusion protein

The first step of the characterization of this mouse model was to see if GFP is even expressed in the first place. After that it made sense to investigate if the GFP is actually part of a GFP-SHANK3 fusion protein instead of just being expressed independently of the SHANK3.

4.2.1 Immunohistochemistry

The immunohistochemical images prove in principal that green fluorescence is produced in the transgenic animal. This can be seen in the undeniable difference of signals in the green fluorescent channels, between the transgenic and the wild type animals.

4.2.2 Western blots

The western blots prove - furthermore - that it is indeed a green fluorescent protein that is producing this fluorescence. Another new piece of information that the western blots provide, is that there is a difference between the animals in regards to the amounts of SHANK3 present in the organisms – namely, that they are higher in the transgenic animals. Inserting an additional gene for the expression of a GFP-SHANK3 fusion protein should lead to a SHANK3 expression that is higher than the amount one would find in a wild type animal. For that reason, the findings of the western blots are in line with our expectations. In both the GFP and SHANK3 blots of figures 9 & 10 there are signals in the transgenic animals at a molecular weight of about 250 kDa. The heaviest isoforms of SHANK3 alone have a molecular weight of 185 - 200 kDa and GFP alone has a molecular weight of 27 kDa (Feilmeier et al., 2000). Since western blots have a very low resolution for proteins on the high end of molecular weights, this is plausibly agreeable with a fusion protein of GFP and SHANK3. However, looking at the GFP blots of figures 9 & 10, one can notice that this is not the only signal. Instead, there are additional signals at molecular weights of approximately 115, 35 and 26 kDa. All of these molecular weights are not agreeable with the weight a GFP-SHANK3 fusion protein would have. Our best putative explanations for the presence of these signals are the following: (1) there are isoforms of the SHANK3 protein that have lower molecular weights (Lim et al., 1999) but still have a GFP attached to them. (2) The GFP-SHANK3 fusion protein is cleaved at different locations, also yielding proteins of lower molecular weight but with a GFP still attached. (3) The GFP-SHANK3 fusion protein is cleaved such that the GFP and the SHANK3 protein are separated from each other. (4) In the process of making the probes for the western blots, the GFP-SHANK3 protein degrades and separates into GFP- and SHANK3-proteins. Since (3) & (4) would produce isolated GFP proteins, these seem like good explanations for the signal at approximately 27 kDa.

4.3 Brain region - specific expression

Now that it had been established as a fact that the expression generally takes place in the transgenic animals, the second step was to see if this expression is limited to certain regions of the brain, or if it is just expressed in its entirety. As already explained, the transactivator controlling the expression of the inserted GFP-Shank3 gene has a CaM kinase II promoter. Because this CaM kinase II promoter is expressed mainly in neurons (Kennedy & Greengard, 1981; Bennett, Erondu & Kennedy, 1983; Kennedy, McGuinness & Greengard, 1983) of the forebrain (Wang et al., 2013), the expectation was that the expression of our fusion protein would also be limited to the same areas.

4.3.1 Immunohistochemistry

The immunohistochemical figures 1, 2 & 3 are a first indicator that the CaM kinase II promoter functions as expected. In them we can find the green fluorescent signal only in (1) the cortex, (2) the Hippocampus and (3) the striatum. All three of these regions are part of the forebrain.

4.3.2 Western blots

For the GFP signal, figure 11A shows no difference between the wildtype and the transgenic animal in the cerebellum and the brain stem. It does, however, show a clear difference in the thalamus, the hippocampus, the striatum and the cortex, namely that the signal is noticeably stronger in the transgenic animals than it is in the wild type animals. This finding supports the conclusion that the CaM kinase II promoter is working as we hoped it would. The SHANK3 signal of Figure 11B shows the same pattern as the GFP signal of figure 11A. This again indicates that it is not only GFP loosely floating around in the cell, but that it seems to be attached to the SHANK3 protein.

4.4 Evidence of the synaptic localization of the GFP-SHANK3 protein

After showing that the CaM kinase II promoter functions as planned, the next step was to decisively see if the GFP-SHANK3 protein is located synaptically, instead of just randomly all over the cell or even in the interstitial space.

4.4.1 Immunohistochemistry

The first conclusion regarding the synaptic localization of the GFP- SHANK3 fusion protein can be drawn from figure 4. In this figure we can see that the green signal is not distributed evenly across the hippocampus, but rather only in specific regions. The noticeably darker areas in the pyramidal cell layer of the CA1-3 regions, as well as in the granular cell region indicate that the signal seems to be coming from the processes of the neurons, rather than their somata. This would be in line with the assumption that the fluorescent signal is coming from a synaptically located GFP- SHANK3 fusion protein, since this would largely exclude an expression around the somata. Figures 5-8 are the main figures concerning this topic. All four of them continue showing only a weak, or even no signal around the somata of the cells. Still the most valuable finding of these figures is, that they clearly show a colocalization of the green GFP- SHANK3 signal with the signal of the presynaptic marker bassoon as well as with the postsynaptic marker SHANK2. This obvious colocalization is strong evidence that our GFP signal locates in the synapse as would be the natural behavior of the SHANK3 protein (Tobias M. Boeckers et al., 1999b; Tobias M Boeckers, Bockmann, Kreutz, & Gundelfinger, 2002). Figure 8 shows the colocalization of the green GFP- SHANK3 signal with the presynaptic marker bassoon in the striatum. This proves that this colocalization is not just an anomalous phenomenon of the hippocampus, but also takes place in the striatum. It is thus more likely to also be the case in other regions of the brain were the fusion protein is expressed. Striatal stainings with the postsynaptic marker SHANK2 were also done, but they did not turn out well.

The SHANK2 signal did not show puncta as a synaptic staining should. It was instead very unspecific and diffuse with sparse filament like structures. The stainings were done again but turned out the same. As to why this was the outcome, our best explanation is that the tissue was not well intact. Perhaps this was due to insufficient perfusion with the PFA fixation solution. Ideally, such staining would be done again at some point.

4.4.2 Western blots

4.4.2.1 Issues with the protein amounts of figures 15 & 16

An issue with the Western blots of figures 15 & 16 that must first be addressed is that of the varying protein amounts. As clearly visible, the actin bands are relatively similar to each other in the lines 1-5. They are then much fainter and also much more variable in the lines after that. The reason for this is that, during the process of cell compartment fractioning, the concentrations of the extracted cell material became smaller and smaller. As a result of this, the concentrations of the compartments Ho, S1, P1 & P2 were diluted to a concentration of 1,125 µg/µL, in order to match the concentrations of the transgenic compartments with those of the wild type compartments. The other fractions however were diluted with the minimum amount necessary so that they could still be used for western blotting. Nonetheless, the differences seem to be slightly larger in the GFP signals, relative to the differences we observe in the β-actin signals. Furthermore, later in sections 4.4.2.5 and 4.4.2.6, I will combine the observations of all the western blots done with the probes of the subcellular fractioning. As a result, these differences in protein amounts will be stripped of their relevance. We had, thus, decided to deem the findings of the subcellular fractionings significant, despite the mostly minor differences in protein amounts.

4.4.2.2 Interpretation of the GFP signals of figure 15B

Regarding the western blots, it is best to begin with the analysis of figure 15B in which we see a GFP signal in different subcellular compartments. The compartments 1-5 (Ho, S1, P1, S2 & P2) all show a strong GFP signal. The Ho fraction represents a homogenate of the entire mouse brain. Not having a signal in this band would have meant that this animal does not express the GFP- SHANK3 fusion protein at all. The S1 fraction represents the homogenate without the nuclei and the cell debris. That still incorporates the synaptosomal fractions, so a signal is to be expected there also. The P1 fraction represents the nuclei and cell debris. The nuclei should not be containing our GFP- SHANK3 fusion protein. The cell debris, per definition, contains unspecific rubble and litter of the cell. Hence, it is well imaginable to find enough GFP epitopes in this fraction to produce a signal in the western blot. The S2 fraction represents the cytosol of the cell. Of these first five bands, the S2 fraction displays the weakest signal. This is a finding that supports the fact that SHANK3 is located at the membranes of the synapses, rather than in the cytosol (Boeckers, 2006). The P2 fraction represents the crude membranes. Since, again, the synaptic membranes is where the GFP- SHANK3 protein should be localized, this finding was as we expected.

The next set of bands that are relevant are the bands 6-9 (Myl, LM, Syn & Mit). Myl represents the myelin fraction. Since myelin is not even inside the neuron, it would not be in line with the expectations of this model if we found a strong signal here. We are therefore pleased to find only a very weak signal in the myelin line. LM represents the light membrane fraction containing the polysomes, the Golgi apparatus, and the smooth endoplasmic reticulum (Taha et al., 2014). Since the light membrane has nothing to do with the synapse, from a standpoint of location, a weak signal here is a pleasant finding. The Syn fraction represents the synaptosome. Because this is precisely where we hope to find our GFP- SHANK3 fusion protein, we gladly report that there is a noticeably stronger signal in this band. The Mit fraction represents the mitochondria. Finding such a strong signal in this band was initially a surprise for us. But, since this initial surprise, have come up with two explanations for this finding: (1) As one can see by looking at the β-actin bands, much more protein was loaded in this line in general. Hence, it would be no surprise to find any signal looking enhanced. (2) The second explanation is the following:

Obviously the mitochondrial fraction is the one where the mitochondria can be found. However, colleagues from my laboratory, who perform PSD-fractionings regularly told me that it is also a fraction were many other components of the cell can be found which are not directly affiliated with the mitochondria. This in turn could be explained by the way the fraction is generated. It is generated by harvesting the material which collects all the way at the bottom of the ultracentrifuge tube after separating P2 in the sucrose gradient. One could imagine that anything, which does not collect at its 'designated' location within the sucrose gradient could simply fall all the way to the bottom of the tube, and thus be collected as part of the mitochondrial fraction.

Lastly, the fractions S3 & P3 must be discussed. The S3 fraction represents the synaptosomal cytosol, whereas the P3 fraction represents the synaptosomal membranes. It is hence a well expected finding to see that the signal in the P3 fraction is clearly visible, while the signal in the S3 fraction is not visible at all.

4.4.2.3 Interpretation of the SHANK3 signals of figure 15A

The main message that the western blot of figure 15A brings forth is that its wild type SHANK3 signal behaves exactly like the transgenic GFP signal of figure 15B. This observation carries valuable information in three regards: (1) The GFP is not merely located at any specific locations inside the cell, but at exactly those where SHANK3 is also located. (2) The comparison with the SHANK3 protein of a wild type animal, instead of the SHANK3 of another transgenic animal, shows that the overlap in subcellular localization is not due to an abnormal Shank3 production which might have occurred in the process of generating these transgenic mice. (3) The differences in protein amounts among the subcellular fractions – as discussed in section 4.4.2.1 – become irrelevant in this context, because the same differences in protein amounts lead to the exact same result in the wild type animal.

4.4.2.4 Interpretation of the SHANK3 and PSD-95 signals of figure 16

As can instantly be seen, both western blots of this figure share the same pattern of signal distribution as both of the western blots of figure 15. As a result, we can retrieve three helpful pieces of information: (1) Figure 16A is another link between the GFP and the SHANK3 in the transgenic animal. Here to, the subcellular expression pattern is very much the same as the one in figure 15B. Therefore, figure 16A serves as one more indicator that the GFP- SHANK3 fusion protein exists in the mouse as such. There may still be loose GFP floating around in the cell, but it is starting to seem more and more undeniable that at least a good part of it is linked to the SHANK3 protein. (2) Figure 16B can be seen as an addition to the comparison of figures 15A & 15B. In that comparison we had established that the GFP expression of figure 15B behaves like that of a postsynaptic protein. Because PSD-95 is also a postsynaptic protein, the same conclusion can be drawn here. Once more, this facilitates the assumption that at least a good amount of GFP is linked to SHANK3. (3) Both the blots of figure 16 show the same pattern of signal distribution, with the same protein amounts in each of the lines as both blots in figure 15. This constitutes the final proof that the differences in protein amounts within the blots – as discussed in section 4.4.2.1 – can confidently be ignored.

4.5 Comparison with the GFP-SHANK3 mouse model of Han et al., 2013

The paper of Han et al., 2013 models the overexpression of SHANK3 in a mouse (Han et al., 2013). Since in principal that is also what we are trying to do, it is important to discuss the similarities of our models and – more importantly – what sets ours apart from the one of Han et al..

4.5.1 Localization

With RNA in situ hybridization against *eGFP*, the group of Han et al. located the EGFP-SHANK3 protein mainly to the cortex, the hippocampus and the striatum. However, since they are still using a physiological *Shank3* gene, the expression cannot possibly be exclusive to these regions. Instead they are merely expressed mostly in these regions, as a normal *Shank3* gene would be. In contrast to that, our group made the expression of the third *Shank3* gene tissue specific by including the CaM kinase II promoter. Our immunohistochemical stainings, as well as our western blots then confirmed a localization at the cortex, the hippocampus and the striatum with the addition of finding an expression in the thalamus.

4.5.2 Reproducibility

At first sight our group did the same thing as the group of Han et al., which was to create an excess of SHANK3. However, when reading the paper of Han et al. closely, one notices that they do not specify exactly how they did this. They write about inserting the EGFP-DNA in front of one of the natural *Shank3*-alleles and then about a following estimated 1.2-fold overexpression. What exactly did they do to initiate this overexpression other than inserting the EGFP-DNA? And why is there even an overexpression in the first place if there are still only two *Shank3* alleles? They do not answer these questions. While it would be nice to give them the benefit of the doubt, the possibility must be entertained that this was not done on purpose, but was more of an accident. Perhaps they simply wanted to fluorescently mark the SHANK3 protein and then coincidentally noticed that there was an overexpression of the gene. So, while their results show that there does seem to be an actual overexpression, and the phenotypes they observed may have been real, it leaves much uncertainty as to the reproducibility of these results. For our project on the other hand, we planned the overexpression on the basis of a solid and validated theoretical background. So even though there is never an absolute guarantee for reproducibility, this makes it incomparably more likely and also gives it a sound and coherent explanation. Therefore, we should be able to reliably produce SHANK3 overexpressing mice in the future, in order to be able to possibly answer new questions that might arise in the years to come.

4.5.3 Future gain of new knowledge

It is also questionable if Han et al.'s model can lead to any following gains of knowledge in the future. For example, the question, if there is a time in the development of the mouse during which the phenotypes can be rescued and if yes when is it? An EGFP tag cannot be inserted or removed simply at any time one wishes. And even if it were possible, it is not clear if this would reliably produce the same results. The conclusion can thus be drawn, that – with this method alone – it is unlikely for Han et al.'s group to make any more progress in this direction. This is where our project really sets itself apart and picks up the pieces. With the tet-off system, the real advantage of our model is that we hope to be able to control the expression. As a result, the plan is to be able to answer said question concerning rescuability during the development of the mouse; the question which Han et al.'s group does not seem to be able to answer.

4.6 Outlook

4.6.1 Novelties & advantages of the system

Leaving the results of the experiments regarding only SHANK3 aside, there is yet still utility in the system of the mouse model itself. For comparison, I will first provide some information about the most popular, and arguably the most versatile system that is currently in actual use, namely the Cre-LoxP system. If not stated otherwise, the information in the following paragraph was derived from Nagy, 2000 as well as Sauer & Henderson 1988 (Nagy, 2000; Sauer & Henderson, 1988). In a nutshell, the system works by inserting LoxP in a palindromic alignment at each end of the DNA segment that is to be manipulated. LoxP stands for 'locus of X-over P1' and it is a DNA-sequence originally derived from bacteria. The act of inserting the LoxP sites itself is called floxing (flanked by loxP). An enzyme called Cre-recombinase then recognizes

the Loxp sites and changes their configuration. A knockout animal can, for example, be created by inserting the LoxP sequences such, that the Cre-recombinase simply removes the DNA in between the LoxP sites. A knockin animal on the other hand could be created by inserting a gene into a chromosome, but oriented in the wrong direction so that it is not functional. In this scenario the Cre-recombinase would switch the orientation of the inserted Gene so that it becomes functional. Other mechanisms are also possible, but I will not go into further detail on all of them. Spatial and temporal control over the process is gained by using Cre genes with tissue specific promoters that can be activated by certain substances (e.g. Tamoxifen (Mei et al., 2016)). The limitation is, that when the Cre-recombinase has served its purpose, the process is not reversible. Also it is an all or nothing event, meaning that the gene is either fully altered or not at all; there is nothing in between. If not stated otherwise, the information of the paragraph above was derived from Nagy, 2000 as well as Sauer & Henderson 1988 (Nagy, 2000; Sauer & Henderson, 1988).

When it comes to the system of the mouse model of this thesis, all the single building blocks used to make it have been known before. The tet-system (Gossen & Bujard, 1992), the technique of inserting genes into the Rosa26 locus, tagging proteins with other fluorescent proteins or making the expression specific to certain tissues, none of these things are inherently new. To our knowledge however, no one has yet created a system combining all these techniques in this specific way. So when it comes to manipulating the function of entire genes, the potential advantages of it over the Cre-LoxP system are twofold: (1) It allows for a quantitative control over the expression of the gene by controlling for the amount of doxycycline given to the animal. (2) Also, the process is reversible, which means for example that if the activity of the gene is downregulated by giving the animal doxycycline, it can be upregulated again by simply giving it less doxycycline. Another feature of the system that will open up quite a lot of doors is the way the targeting construct was constructed. Usually, making such a targeting construct involves inserting all the pieces (such as the long arm of the Rosa26 locus, the short arm of the locus, the promoter, the desired gene, etc.) step by step, in a process that can easily take up to a year to complete. While all of this was also done for our targeting construct, additional two attachment sites were inserted (see figure 1). These attachment sites are part of the Gateway® - system of the company Invitrogen – life technologies. The enzyme mix contains enzymes that can recombine the attachment sites with others, similar to the Cre-recombinase system. This

allows us to extract the cassette containing the DNA for the GFP-*Shank3* gene and to insert any new cassette that we want practically overnight. This way, similar experiments can be done with any other genes/proteins without having to wait up to a year for any single new mouse model.

4.6.2 Disadvantage of the system

4.6.2.1 Regional limitations of GFP- SHANK3 expression

The CaM kinase II promoter is important for limiting the overexpression to the brain, instead of expressing the *GFP-Shank3* gene in every cell of the body. The downside to this is that the promoter does not only limit the expression to the brain, but also to certain parts of the brain, namely the forebrain. Natural SHANK3 however is found in the forebrain in larger amounts than in other regions, but it is not exclusive to it. We assume and hope that SHANK3 expression limited to the forebrain should be sufficient to produce a phenotype that would be at least very similar to that of a natural SHANK3 overexpression. It could however be argued that this might not necessarily be the case. To control for this, behavioral studies could be done. The data from these behavioral studies could then be compared to that of Han et al. 2013, since their mice overexpress a natural *Shank3* gene. Another question one might ask is why we even used a CaM kinase II promoter instead of a natural *Shank3* promoter in the first place? Experience has shown that inserting DNA coding for a fluorescent protein in between the DNA of a protein and its natural promoter often leads to a low quantity of expression. This could possibly produce mice with only a mild phenotype. Unfortunately, that would not show us the entire picture of the consequences of SHANK3 overexpression. Also it would give us only a small range for the tet-system to operate in. Additionally, it would make it harder to detect the fluorescent signal under the microscope. Thus, the purpose of the project would mostly be defeated. The CaM kinase II promoter on the other hand is one of the most abundant proteins in the postsynaptic density (Yoshimura et al., 2002). Therefore, one can imagine the expression to be quite strong, which has been the experience of colleagues in our laboratory. It is therefore sort of an insurance for the function of our mouse model. In any case, the forebrain nicely covers the main regions in

which natural SHANK3 is located. Therefore, we believe that this model will be sufficient to move us forward on the quest for new knowledge in this area.

4.6.2.2 Toxicity of doxycycline

One question that can and should be raised concerns potential toxic effects of doxycycline on the mouse organism. A quick and relatively decisive answer to this question is that toxicity has not yet been reported in mice (Redelsperger et al., 2016). However, the group of Redelsperger et al. notes that there might have been cases of gastrointestinal inflammation in some of their mice receiving especially high doses of doxycycline. The paper states that there are no official recommendations concerning doxycycline dosages in mutant mice with tet-systems. But it also suggests, that some tissues (such as brain tissue) may need higher concentrations of doxycycline. Since brain tissue is exactly the one we are analyzing in this project, it must be taken into consideration that this might pose an issue for us. To solve this, a two-step experiment could be done: (1) We could first experiment on the doxycycline concentrations necessary to produce the desired differences in the GFP- SHANK3 expression. Once that is established (2) we could compare wild type mice treated with that doxycycline dosage to wild type mice that are completely untreated. It would be important to compare to wild type mice to each other in the second step of this experiment. If transgenic animals were used, we would not know if any potentially toxic effects are due to the doxycycline itself or to the lower levels of SHANK3 it induces. This way we could find out if the dosages of doxycycline, which are necessary to sufficiently inhibit GFP- SHANK3 expression, have any negative effects on the mice.

4.6.3 SHANK3 Isoforms

There at least five intragenic promoters which lead to promoter specific isoforms that can have many different combinations of functional domains. Additionally, there is a high level of activity regarding alternative spicing. These factors lead to a large number of different isoforms of the

SHANK3 protein with distinct functions. Not only are there many isoforms, but they are also represented in varying quantities in different brain regions as well as in different subcellular compartments. Additionally, different isoforms are expressed in different levels during the course of the development. Furthermore, expression seems to be dependent on the general activity of the neuron itself. Lastly, it seems to be the case that epigenetic factors may also play a role in the expression (Wang, Xu, Bey, Lee, & Jiang, 2014). A factor in the mouse model of this thesis, which must be considered, is that our inserted *SHANK3* gene does not necessarily behave like a natural *SHANK3* gene at all. In the future, it might therefore possibly be necessary to investigate into the behavior of our inserted *SHANK3* gene regarding (1) the variety of isoforms produced, (2) their distribution within the brain and the cell and (3) the fact that the expression of the inserted *SHANK3* gene is not dependent on stages of development, neuronal activity or epigenetic factors.

4.6.4 Titration

The next step of this project is the titration project. Since a major part of this mouse model is the tet-off system, its function must also be tested. This will be done by giving the mice doxycycline in different doses and then doing western blots and immunohistochemistry in order to verify if the doxycycline led to a decrease, or even a total absence of the GFP-SHANK3 protein. Some of these experiments have already been done and the still unpublished data shows that the GFP-Protein is downregulated when the animals are given doxycycline.

4.6.5 Future projects

4.6.5.1 Rescue

The group of Han et al. did behavioral tests with their mice in order to find out what the phenotype of SHANK3 overexpressing animals looks like. So since this has now been shown, it would be pointless for our group to simply repeat these experiments for reasons other than

validating our own model, as discussed in section 4.7.1. But, if the tet-off system proves to be functional and our group is able to control the levels of SHANK3 overexpression, there would be a new reason to do behavioral tests. This brings us back to the advantage of our model over that of Han et al.'s group, namely that we could investigate a rescue of the SHANK3 overexpressing animals' phenotype. What this could mean concretely is, that the overexpression could be stopped at different time points of the animals' development and then behavioral tests could be done to verify if the phenotypes of hyperkinesia and decreased social interaction – as reported by Han et al. 2013 – disappear. The information provided by such an experiment could answer three questions: (1) Is the phenotype produced by the overexpression of SHANK3 rescuable at all? (2) Is there a point during the development of the mice after which the phenotype can no longer be rescued? And (3) if there is such a point during the development, when is it exactly? There is good reason to believe that the first two questions will be answered with a yes. This is because the group of Mei et al., 2016 has already rescued the phenotype of a mouse model under expressing SHANK3 in a knockdown background. The group has also shown that there seems to be a critical time window during which normal SHANK3 levels must be restored in order to not have a phenotype in the animals. It thus seems probable that these findings would be the similar in an overexpressing animal, but of course one cannot know for sure without testing for it. For comparability reasons it would make sense to execute some of the same behavioral tests as Han et al.'s group did. These could include: (1) the open field test, (2) home-cage activity, (3) the tail suspension test, (4) acoustic startle response and prepulse inhibition, (5) circadian rhythms, (6) the three chamber test, (7) grooming behavior, (8) ultrasonic vocalization, (9) EEG measurement and (10) drug treatment with amphetamines, lithium and valproate (Han et al., 2013).

4.6.5.2 Crossing with *Shank3*$^{+/-}$

In the far future – if everything works out for the best – our group could attempt to create a conditional knockout model. This could be done by crossing our conditional knockin animal with a *Shank3*$^{+/-}$ animal. In the best case scenario this would yield a mouse with one physiological *Shank3* allele and one *Shank3* gene controlled by the CaM kinase II transactivator,

which can be inhibited by doxycycline. Since the group of Mei et al. has already created a conditional *Shank3* knockout model, the differences between their model and our potential future model must be discussed: Mei et al.'s group created a model with the Cre-dependent genetic switch (FLEx) strategy, such that – in the absence of Cre – the animals function as *Shank3* knockout animals. In order to be able to control the re-expression of SHANK3, they crossed this animal with an inducible CAGGS-CreER mouse line which activates the Cre function when tamoxifen is given to the animal. They then gave tamoxifen to the animals at ages between 2 and 4.5 months and found that they could restore some of the aspects of biochemistry, physiology and behavior, but not others. The restorable aspects were: (1) biochemical makeup of major proteins responsible for scaffolding and signaling within the striatum, (2) striatal electrophysiology, (3) striatal spine density, (4) repetitive overgrooming and (5) deficits in social interaction. Not only do these findings show that there are conditions of SHANK3 deficient mice that are restorable, but that they are restorable even as late as in adulthood. This – Mei et al.'s group claims – had not been shown before. Nonetheless, there were also behavioral aspects that were not restorable. These were: (1) exploratory behavior, (2) anxiety-like behavior and (3) motor coordination deficits. The group of Mei et al. wanted to know if the fact that they could not restore these behavioral deficits was because they had missed a critical time point during the development of the mice, after which they are not restorable. To investigate this, they restored the SHANK3 expression at the germline stage and found that these animals had no deficits at all when compared to the wild type mice. This indeed indicates that there probably is a critical point in time before which SHANK3 levels must be restored for the animals to not produce any phenotypes. In order to go even further into this matter, they treated mice with tamoxifen at P20-21. They found that the previously unrestorable anxiety-like behavior, as well as the motor coordination deficits were significantly reduced. The fact that they were reduced but did not fully disappear leads to an interesting conclusion: Figure 17 shows two hypothetical ways of seeing the relationship between the age of the mouse at the time of SHANK3 restoration and the perseverance of phenotypes after the restoration. Figure 17A shows the relationship as a gradual process with the perseverance of phenotypes decreasing with lower age of the mouse (the different functions are variations of possible relationships). Figure 17B shows an all or nothing relationship, with all phenotypes persevering after a certain age at which SHANK3 levels are restored. The paper of Mei et al. now suggests that the reality seems to be better represented by figure 17A. Either way, both scenarios would yield an age before

which SHANK3 levels must be restored in order to rescue all phenotypes in the animals. Unfortunately, the group did not do further experiments in order to find out when exactly this critical age is. All they did in this regard was to determine that it must be some time before P20-21. Finally, this is where our potential future conditional knockout animal model could come in to play a part, namely at answering that question which was left unanswered by Mei et al.'s group: When is the age of the developing mouse before which restoration of physiological SHANK3 levels fully restores all phenotypes?

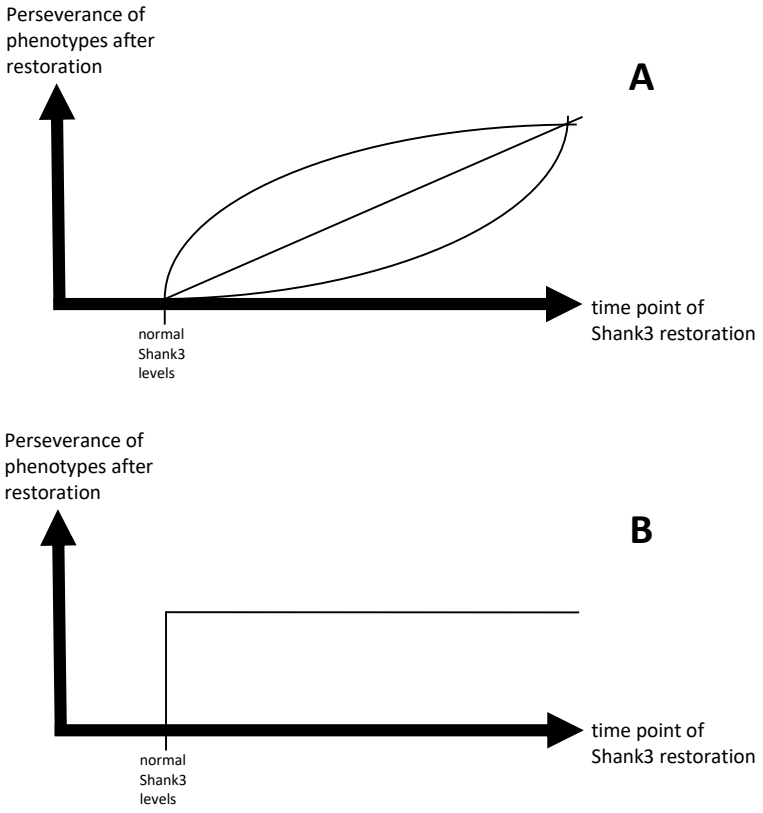

Figure 16: Two possible and hypothetical relationships between the age at which physiological Shank3 levels are restored in the organism of a mouse and the severity of phenotypes that persevere after restoration

4.6.5.3 Trauma

In the Institute for Anatomy and Cell biology of Ulm University, there are studies being done on the question: What happens to SHANK3 in the brain after trauma, and what phenotypes result from that. If this project yields mentionable results, this very mouse model could then later be used to reintroduce SHANK3 to the brain after trauma. Then observations could be made as to the reversibility of any deficits produced by said trauma. This could be done by inhibiting the expression of our inserted *Shank3* allele by giving the mouse doxycycline and activating the expression after the trauma by ending the delivery of doxycycline. In the future, the knowledge gained from such an experiment could give insight as to the worthwhileness of possibly somehow substituting SHANK3 in posttraumatic patients.

4.6.5.4 Amyotrophic lateral sclerosis (ALS)

Another group in our institute is studying the effects of heterozygous and homozygous TBK1 knockout animals on muscle cells and neurons in cell culture. They take keratinocytes from the hair of human patients, dedifferentiate them into induced pluripotent stem cells. Then they induce differentiation into neurons and muscle cells in order to mimic the motor end plate. The aims are (1) to generally study the effects of the different TBK1 knockouts and (2) to gain new information on the question if ALS is a disease of the motor neurons causing the muscle to degenerate – as is the current state of knowledge – or if it may actually be a disease of the muscle cell itself, in turn causing the neuron to degenerate. If actual new knowledge is generated on these questions, it could make sense to confirm those results *in vivo*. To do this, they could use our new system to quickly and easily insert a cassette with the TKB1 gene into our targeting construct and insert it into a TBK1 knockout mouse. This way they could elegantly study the effects of a lack of TBK1 in a mouse model.

4.6.6 Relevance to humans

The ultimate end goal of any scientific endeavor is of course to find an application to actual human life. Because this study is no different, it will be worthwhile to elaborate on the real life utility of this project: As a reminder, the prevalence of ASD is about 1% - 2%. (Park et al., 2016) and of all ASD cases, *Shank3* mutations are responsible for 0.69% (Leblond et al., 2014). Most of these 0.69% are SHANK3 deficiencies, while only very few owe their problems to an excess of SHANK3. Even though this study is about SHANK3 overexpression, there is still potential utility for the cases of under-expression. For example, one could imagine a future scenario in which SHANK3 deficiencies are substituted somehow. The fact that an excess of SHANK3 leads to pathological phenotypes (Durand et al., 2007) shows that a substitution would have to be done in just the right dosage. Thus, studying the physiology of SHANK3 overexpression could give insights as to the quantitative and temporal limits of such a substitution. Regarding the overexpression, I found information on three patients: (1) The first is a boy with 22qter partial trisomy which lead to an additional copy of 22q13. The disease was inherited from a paternal translocation. He has Asperger syndrome with normal language abilities but severely impaired social communication (Durand et al., 2007). (2) The second is a girl with a partial 22q13.3 trisomy, which was also inherited from a paternal translocation. She has ADHD and mild cognitive impairment (Moessner et al., 2007). (3) Lastly, there is a girl with a 22q13.3-qter duplication who has schizophrenia. It is not clear if this was a *de novo* mutation or if it was inherited because the parents are not alive (Failla et al., 2007). Obviously this study alone will not lead to finding a cure for these patients. Nonetheless, it is a small stepping stone on the way to getting there.

4.6.7 Conclusions

The model has thus far proven to be functional as planned. Immunohistochemical methods and western blots were used to verify this. They showed that the expression of the GFP- SHANK3 protein takes place in the mouse brain. The expression is specific to hippocampus, striatum,

thalamus and cortex, which is proof that the CaM kinase II promoter is functional as planned. They also showed that the expression takes place at the synapse, where SHANK3 is naturally localized. A comparison with the publication of Han et al. 2013 shows that, even though the topic is similar at first sight, their project leaves many questions unanswered and seems to have arrived at a dead end. This leaves much potential for our project to be beneficial in the future. The system used to control genetic expression in our mice is new and may lead to answering questions difficult to answer in the past. It may also make it easier to genetically engineer mice in the future, potentially enabling even faster progress in the field of mouse modeling in general. Disadvantages of the system were presented, with suggestions for possible solutions. An elaboration on potential future experiments further facilitates the usefulness of this thesis. Lastly, connections to real human cases were made, validating the utility of this project and this direction of research in general.

5. Summary

As the name conveys, autism spectrum disorder (ASD) is not a single disease, but rather an umbrella term for many different phenotypes. They can differ in many regards such as hyperactivity, epilepsy or intellectual disability. However, to be placed under the label of ASD they all must have two criteria in common: (1) limited and stereotypical patterns of activities and interests, as well as (2) deficits in social communication and interaction. The vast heterogeneity of the disorder is due to its many causal factors, 80 – 90 % of which still are not known. The remaining 10 – 20 % have been linked to genetic causes. Of all ASD cases, 0.69 % have a *Shank3* mutation as the underlying cause. The main function of SHANK3 in the brain is that of a scaffolding protein. It creates a meshwork for many other proteins to bind to and it connects the postsynaptic membrane to the cytoskeleton, structurally as well as functionally. The topic of this thesis specifically is the overexpression of SHANK3. The specific phenotypes of SHANK3 overexpression have been modeled in mice before. They display manic-like behavior, epileptic seizures, hyperkinetic disorders, anxiety and – in contrast to *Shank3*-knockout animals – there is no repetitive behavior. We have created a new system for modeling the overexpression of SHANK3 in mice and one of the two main goals of this thesis is to find out if it is functional as the design intends. What is new about this model is a combination of known techniques. The gene was inserted into the Rosa26 locus with two attachment sites. These attachment sites make it easy to extract the gene and to insert any new gene in a very short time. The gene we inserted for this project is one coding for a GFP-SHANK3 protein. The promoter is a CaM kinase II promoter, which limits the expression to the forebrain. This is not exclusively where natural SHANK3 is expressed, but it is expressed mainly in those brain regions. The promoter is further regulated by a tet-off system. In our case this means that the presence of doxycycline inhibits the expression of the gene, while it expresses freely as long as doxycycline is not present. The group of Han et al. 2013 was the first to specifically model the overexpression of SHANK3 in mice. However, the group of Han et al. seems to have created their mouse model quite coincidentally. Hence, the reproducibility, and therefore the investigation of any further questions on their part seems questionable. These further questions are: (1) Are the phenotypes of the overexpressing mice reversible if SHANK3 levels are normalized? (2) Is there an age of the developing mice, before which this normalization must

take place in order to restore all the phenotypes? (3) If there is such a critical age, when is it? Those questions will not be answered in this thesis, but are still listed for validation of the utility of the project. The methods employed to characterize the mouse model were immunohistochemistry and western blotting. Both methods reveal an undeniable difference between the GFP signals of the transgenic animals and the wild type animals. The immunohistochemical stainings showed green fluorescent signals limited to the cortex, the hippocampus and the striatum. While the western blots did the same, they additionally showed a GFP signal in the thalamus. Since these are all part of the forebrain this validates the functionality of the CaM kinase II promoter–controlled transactivator. Within these brain regions, further stainings showed these green fluorescent signals to colocalize with the presynaptic marker bassoon and with the postsynaptic marker SHANK2. Western blots also pinned the GFP signal down mostly to the subcellular fraction of the synaptosomal membrane. Furthermore, the western blots reveal that the expression of the GFP signal behaves exactly like that of other postsynaptic proteins in wild types (namely SHANK3 and PSD-95). Since SHANK3 is a postsynaptic protein, our GFP-SHANK3 protein should also localize postsynaptically. This expectation is confirmed by said stainings and blots. It can thus be concluded, that the mouse model is functional as planned, in regards to the expression and localization of the GFP-SHANK3 fusion protein.

6. Reference list

1. Allen Institute for Brain Science
http://atlas.brain-map.org/ (28.09.2018)

2. Alonso, C. (2013). An Overview of Stimulated Emission Depletion (STED) Microscopy and Applications. *Journal of Lower Genital Tract Disease*, *14*(3), 248–252. https://doi.org/10.1097/LGT.0b013e3181eb2087

3. Amaral, D. G., Schumann, C. M., & Nordahl, C. W. (2008). Neuroanatomy of autism. *Trends in Neurosciences*, *31*(3), 137–145. https://doi.org/10.1016/j.tins.2007.12.005

4. American psychiatric association, DSM – 5 fact sheet, autism spectrum disorder https://www.psychiatry.org/psychiatrists/practice/dsm/educational-resources/dsm-5-fact-sheets (28.09.2018)

5. Baron, M. K., Boeckers, T. M., Vaida, B., Faham, S., Gingery, M., Sawaya, M. R., … Bowie, J. U. (2006). An architectural framework that may lie at the core of the postsynaptic density. *Science (New York, N.Y.)*, *311*(5760), 531–535. https://doi.org/10.1126/science.1118995

6. Bennett, M. K., Erondu, N. E., & Kennedy, M. B. (1983). Purification and characterization of a calmodulin-dependent protein kinase that is highly concentrated in brain. *The Journal of Biological Chemistry*, *258*(20), 12735–12744. Retrieved from http://www.ncbi.nlm.nih.gov/pubmed/6313675

7. Berg, E. L., Copping, N. A., Rivera, J. K., Pride, M. C., Careaga, M., Bauman, M. D., … Silverman, J. L. (2018). Developmental social communication deficits in the Shank3 rat model of phelan-mcdermid syndrome and autism spectrum disorder. *Autism Research : Official Journal of the International Society for Autism Research*, *11*(4), 587–601. https://doi.org/10.1002/aur.1925

8. Berkel, S., Marshall, C. R., Weiss, B., Howe, J., Roeth, R., Moog, U., … Rappold, G. A. (2010). Mutations in the SHANK2 synaptic scaffolding gene in autism spectrum disorder and mental retardation. *Nature Genetics*, *42*(6), 489–491. https://doi.org/10.1038/ng.589

9. Berkel, S., Tang, W., Treviño, M., Vogt, M., Obenhaus, H. A., Gass, P., … Rappold, G. A. (2012). Inherited and de novo SHANK2 variants associated with autism spectrum disorder impair neuronal morphogenesis and physiology. *Human Molecular Genetics*, *21*(2), 344–357. https://doi.org/10.1093/hmg/ddr470

10. Betancur, C. (2011). Etiological heterogeneity in autism spectrum disorders: more than 100 genetic and genomic disorders and still counting. *Brain Research*, *1380*, 42–77. https://doi.org/10.1016/j.brainres.2010.11.078

11. Böckers, T. M., Mameza, M. G., Kreutz, M. R., Bockmann, J., Weise, C., Buck, F., … Kreienkamp, H. J. (2001). Synaptic scaffolding proteins in rat brain. Ankyrin repeats of the multidomain Shank protein family interact with the cytoskeletal protein alpha-fodrin. *The Journal of Biological Chemistry*, *276*(43), 40104–40112. https://doi.org/10.1074/jbc.M102454200

12. Bockmann, J., Kreutz, M. R., Gundelfinger, E. D., & Böckers, T. M. (2002). ProSAP/Shank postsynaptic density proteins interact with insulin receptor tyrosine kinase substrate IRSp53. *Journal of Neurochemistry*, *83*(4), 1013–1017. https://doi.org/1204 [pii]

13. Boeckers, T. M., Kreutz, M. R., Winter, C., Zuschratter, W., Smalla, K. H., Sanmarti-Vila, L., … Gundelfinger, E. D. (1999a). Proline-rich synapse-associated protein-1/cortactin binding protein 1 (ProSAP1/CortBP1) is a PDZ-domain protein highly enriched in the postsynaptic density. *The Journal of Neuroscience : The Official Journal of the Society for Neuroscience*, *19*(15), 6506–6518. https://doi.org/10.1016/S0940-9602(01)80024-8

14. Boeckers, T. M., Winter, C., Smalla, K. H., Kreutz, M. R., Bockmann, J., Seidenbecher, C., … Gundelfinger, E. D. (1999b). Proline-rich synapse-associated proteins ProSAP1 and ProSAP2 interact with synaptic proteins of the SAPAP/GKAP family. *Biochemical and Biophysical Research Communications*, *264*(1), 247–252. https://doi.org/10.1006/bbrc.1999.1489

15. Boeckers, T. M., Bockmann, J., Kreutz, M. R., & Gundelfinger, E. D. (2002). ProSAP/Shank proteins - a family of higher order organizing molecules of the postsynaptic density with an emerging role in human neurological disease. *Journal of Neurochemistry*, *81*(5), 903–910. Retrieved from http://www.ncbi.nlm.nih.gov/pubmed/12065602

16. Boeckers, T. M. (2006). The postsynaptic density. *Cell and Tissue Research*, *326*(2), 409–422. https://doi.org/10.1007/s00441-006-0274-5

17. Chang, J.-B., Chen, F., Yoon, Y.-G., Jung, E. E., Babcock, H., Kang, J. S., … Boyden, E. S. (2017). Iterative expansion microscopy. *Nature Methods*, *14*(6), 593–599. https://doi.org/10.1038/nmeth.4261

18. Chen, F., Tillberg, P. W., & Boyden, E. S. (2015). Optical imaging. Expansion microscopy. *Science (New York, N.Y.)*, *347*(6221), 543–548. https://doi.org/10.1126/science.1260088

19. Chung, K., Wallace, J., Kim, S.-Y., Kalyanasundaram, S., Andalman, A. S., Davidson, T. J., … Deisseroth, K. (2013). Structural and molecular interrogation of intact biological systems. *Nature*, *497*(7449), 332–337. https://doi.org/10.1038/nature12107

20. de Wet, J. R., Wood, K. V, DeLuca, M., Helinski, D. R., & Subramani, S. (1987). Firefly luciferase gene: structure and expression in mammalian cells. *Molecular and Cellular Biology*, *7*(2), 725–737. https://doi.org/10.1128/MCB.7.2.725.Updated

21. Durand, C. M., Betancur, C., Boeckers, T. M., Bockmann, J., Chaste, P., Fauchereau, F., … Bourgeron, T. (2007). Mutations in the gene encoding the synaptic scaffolding protein SHANK3 are associated with autism spectrum disorders. *Nature Genetics*, *39*(1), 25–27. https://doi.org/10.1038/ng1933

22. Failla, P., Romano, C., Alberti, A., Vasta, A., Buono, S., Castiglia, L., … Galesi, O. (2007). Schizophrenia in a patient with subtelomeric duplication of chromosome 22q. *Clinical Genetics*, *71*(6), 599–601. https://doi.org/10.1111/j.1399-0004.2007.00819.x

23. Feilmeier, B. J., Iseminger, G., Schroeder, D., Webber, H., & Phillips, G. J. (2000). Green fluorescent protein functions as a reporter for protein localization in Escherichia coli. *Journal of Bacteriology*, *182*(14), 4068–4076. https://doi.org/10.1128/JB.182.14.4068-4076.2000

24. Friedrich, G., & Soriano, P. (1991). Promoter traps in embryonic stem cells: a genetic screen to identify and mutate developmental genes in mice. *Genes & Development*, *5*(9), 1513–1523. https://doi.org/10.1101/gad.5.9.1513

25. Gossen, M., & Bujard, H. (1992). Tight control of gene expression in mammalian cells by tetracycline-responsive promoters. *Proceedings of the National Academy of Sciences of the United States of America*, *89*(12), 5547–5551. https://doi.org/10.1073/pnas.89.12.5547

26. Gould, S. J., & Subramani, S. (1988). Firefly luciferase as a tool in molecular and cell biology. *Analytical Biochemistry*, *175*(1), 5–13. https://doi.org/10.1016/0003-2697(88)90353-3

27. Halbedl, S., Schoen, M., Feiler, M. S., Boeckers, T. M., & Schmeisser, M. J. (2016). Shank3 is localized in axons and presynaptic specializations of developing hippocampal neurons and involved in the modulation of NMDA receptor levels at axon terminals. *Journal of Neurochemistry*, *137*(1), 26–32. https://doi.org/10.1111/jnc.13523

28. Han, K., Holder, J. L., Schaaf, C. P., Lu, H.-C., Chen, H., Kang, H., … Zoghbi, H. Y. (2013). SHANK3 overexpression causes manic-like behaviour with unique pharmacogenetic properties. *Nature*, *503*(7474), 72–77. https://doi.org/10.1038/nature12630

29. Heise, C., Schroeder, J. C., Schoen, M., Halbedl, S., Reim, D., Woelfle, S., … Boeckers, T. M. (2016). Selective Localization of Shanks to VGLUT1-Positive Excitatory Synapses in the Mouse Hippocampus. *Frontiers in Cellular Neuroscience*, *10*, 106. https://doi.org/10.3389/fncel.2016.00106

30. Hell, S. W. (2007). Far-field optical nanoscopy. *Science (New York, N.Y.)*, *316*(5828), 1153–1158. https://doi.org/10.1126/science.1137395

31. Jiang, Y.-H., & Ehlers, M. D. (2013). Modeling autism by SHANK gene mutations in mice. *Neuron*, *78*(1), 8–27. https://doi.org/10.1016/j.neuron.2013.03.016

32. Kennedy, M. B., & Greengard, P. (1981). Two calcium/calmodulin-dependent protein kinases, which are highly concentrated in brain, phosphorylate protein I at distinct sites. *Proceedings of the National Academy of Sciences of the United States of America*, *78*(2), 1293–1297. https://doi.org/10.1073/pnas.78.2.1293

33. Kennedy, M. B., McGuinness, T., & Greengard, P. (1983). A calcium/calmodulin-dependent protein kinase from mammalian brain that phosphorylates Synapsin I: partial purification and characterization. *The Journal of Neuroscience : The Official Journal of the Society for Neuroscience*, *3*(4), 818–831. Retrieved from http://www.ncbi.nlm.nih.gov/pubmed/6403674

34. Kolevzon, A., Angarita, B., Bush, L., Wang, A. T., Frank, Y., Yang, A., … Buxbaum, J. D. (2014). Phelan-McDermid syndrome: a review of the literature and practice parameters for medical assessment and monitoring. *Journal of Neurodevelopmental Disorders*, *6*(1), 39. https://doi.org/10.1186/1866-1955-6-39

35. Kreienkamp, H. J., Zitzer, H., Gundelfinger, E. D., Richter, D., & Bockers, T. M. (2000). The calcium-independent receptor for alpha-latrotoxin from human and rodent brains interacts with members of the ProSAP/SSTRIP/Shank family of multidomain proteins. *The Journal of Biological Chemistry*, *275*(42), 32387–32390. https://doi.org/10.1074/jbc.C000490200

36. Lai, M.-C., Lombardo, M. V., Ruigrok, A. N. V, Chakrabarti, B., Wheelwright, S. J., Auyeung, B., … Baron-Cohen, S. (2012). Cognition in males and females with autism: similarities and differences. *PloS One*, *7*(10), e47198. https://doi.org/10.1371/journal.pone.0047198

37. Leblond, C. S., Nava, C., Polge, A., Gauthier, J., Huguet, G., Lumbroso, S., … Bourgeron, T. (2014). Meta-analysis of SHANK Mutations in Autism Spectrum Disorders: a gradient of severity in cognitive impairments. *PLoS Genetics*, *10*(9), e1004580. https://doi.org/10.1371/journal.pgen.1004580

38. Lilja, J., Zacharchenko, T., Georgiadou, M., Jacquemet, G., De Franceschi, N., Peuhu, E., … Ivaska, J. (2017). SHANK proteins limit integrin activation by directly interacting with Rap1 and R-Ras. *Nature Cell Biology*, *19*(4), 292–305. https://doi.org/10.1038/ncb3487

39. Lim, S., Naisbitt, S., Yoon, J., Hwang, J. I., Suh, P. G., Sheng, M., & Kim, E. (1999). Characterization of the Shank family of synaptic proteins. Multiple genes, alternative splicing, and differential expression in brain and development. *The Journal of Biological Chemistry*, *274*(41), 29510–29518. https://doi.org/10.1074/JBC.274.41.29510

40. Lim, S., Sala, C., Yoon, J., Park, S., Kuroda, S., Sheng, M., & Kim, E. (2001). Sharpin, a novel postsynaptic density protein that directly interacts with the shank family of proteins. *Molecular and Cellular Neurosciences*, *17*(2), 385–397. https://doi.org/10.1006/mcne.2000.0940

41. Mei, Y., Monteiro, P., Zhou, Y., Kim, J.-A., Gao, X., Fu, Z., & Feng, G. (2016). Adult restoration of Shank3 expression rescues selective autistic-like phenotypes. *Nature*, *530*(7591), 481–484. https://doi.org/10.1038/nature16971

42. Moessner, R., Marshall, C. R., Sutcliffe, J. S., Skaug, J., Pinto, D., Vincent, J., … Scherer, S. W. (2007). Contribution of SHANK3 Mutations to Autism Spectrum Disorder. *The American Journal of Human Genetics*, *81*(6), 1289–1297. https://doi.org/10.1086/522590

43. Nagy, A. (2000). Cre recombinase: the universal reagent for genome tailoring. *Genesis (New York, N.Y. : 2000)*, *26*(2), 99–109. https://doi.org/10.1002/(SICI)1526-968X(200002)26:2<99::AID-GENE1>3.0.CO;2-B

44. Naisbitt, S., Eunjoon, K., Tu, J. C., Xiao, B., Sala, C., Valtschanoff, J., … Sheng, M. (1999). Shank, a novel family of postsynaptic density proteins that binds to the NMDA receptor/PSD-95/GKAP complex and cortactin. *Neuron*, *23*(3), 569–582. https://doi.org/10.1016/S0896-6273(00)80809-0

45. Nickl-Jockschat, T., & Michel, T. M. (2011). The role of neurotrophic factors in autism. *Molecular Psychiatry*, *16*(5), 478–490. https://doi.org/10.1038/mp.2010.103

46. Park, E., Na, M., Choi, J., Kim, S., Lee, J.-R., Yoon, J., … Kim, E. (2003). The Shank family of postsynaptic density proteins interacts with and promotes synaptic accumulation of the beta PIX guanine nucleotide exchange factor for Rac1 and Cdc42. *The Journal of Biological Chemistry*, *278*(21), 19220–19229. https://doi.org/10.1074/jbc.M301052200

47. Park, H. R., Lee, J. M., Moon, H. E., Lee, D. S., Kim, B.-N., Kim, J., … Paek, S. H. (2016). A Short Review on the Current Understanding of Autism Spectrum Disorders. *Experimental Neurobiology*, *25*(1), 1–13. https://doi.org/10.5607/en.2016.25.1.1

48. Peça, J., Feliciano, C., Ting, J. T., Wang, W., Wells, M. F., Venkatraman, T. N., … Feng, G. (2011). Shank3 mutant mice display autistic-like behaviours and striatal dysfunction. *Nature*, *472*(7344), 437–442. https://doi.org/10.1038/nature09965

49. Phelan, K., & McDermid, H. E. (2012). The 22q13.3 Deletion Syndrome (Phelan-McDermid Syndrome). *Molecular Syndromology*, *2*(3–5), 186–201. https://doi.org/000334260

50. Ponna, S. K., Myllykoski, M., Boeckers, T. M., & Kursula, P. (2017). Structure of an unconventional SH3 domain from the postsynaptic density protein Shank3 at ultrahigh resolution. *Biochemical and Biophysical Research Communications*, *490*(3), 806–812. https://doi.org/10.1016/j.bbrc.2017.06.121

51. Qualmann, B., Boeckers, T. M., Jeromin, M., Gundelfinger, E. D., & Kessels, M. M. (2004). Linkage of the actin cytoskeleton to the postsynaptic density via direct interactions of Abp1 with the ProSAP/Shank family. *The Journal of Neuroscience : The Official Journal of the Society for Neuroscience*, *24*(10), 2481–2495. https://doi.org/10.1523/JNEUROSCI.5479-03.2004

52. Redelsperger, I. M., Taldone, T., Riedel, E. R., Lepherd, M. L., Lipman, N. S., & Wolf, F. R. (2016). Stability of Doxycycline in Feed and Water and Minimal Effective Doses in Tetracycline-Inducible Systems. *Journal of the American Association for Laboratory Animal Science : JAALAS*, *55*(4), 467–474. Retrieved from http://www.ncbi.nlm.nih.gov/pubmed/27423155

53. Sala, C., Piëch, V., Wilson, N. R., Passafaro, M., Liu, G., & Sheng, M. (2001). Regulation of dendritic spine morphology and synaptic function by Shank and Homer. *Neuron*, *31*(1), 115–130. https://doi.org/10.1016/S0896-6273(01)00339-7

54. Sauer, B., & Henderson, N. (1988). Site-specific DNA recombination in mammalian cells by the Cre recombinase of bacteriophage P1. *Proceedings of the National Academy of Sciences of the United States of America*, *85*(14), 5166–5170. https://doi.org/10.1073/pnas.85.14.5166

55. Schmeisser, M. J., Ey, E., Wegener, S., Bockmann, J., Stempel, A. V., Kuebler, A., … Boeckers, T. M. (2012). Autistic-like behaviours and hyperactivity in mice lacking ProSAP1/Shank2. *Nature*, *486*(7402), 256–260. https://doi.org/10.1038/nature11015

56. Sheng, M., & Kim, E. (2000). The Shank family of scaffold proteins. *Journal of Cell Science*, *113 (Pt 1*, 1851–1856. Retrieved from http://www.ncbi.nlm.nih.gov/pubmed/10806096

57. Soltau, M., Richter, D., & Kreienkamp, H.-J. (2002). The insulin receptor substrate IRSp53 links postsynaptic shank1 to the small G-protein cdc42. *Molecular and Cellular Neurosciences*, *21*(4), 575–583. https://doi.org/10.1006/mcne.2002.1201

58. Taha, M. S., Nouri, K., Milroy, L. G., Moll, J. M., Herrmann, C., Brunsveld, L., … Ahmadian, M. R. (2014). Subcellular fractionation and localization studies reveal a direct interaction of the fragile X mental retardation protein (FMRP) with nucleolin. *PLoS ONE*. https://doi.org/10.1371/journal.pone.0091465

59. Tillberg, P. W., Chen, F., Piatkevich, K. D., Zhao, Y., Yu, C.-C. J., English, B. P., … Boyden, E. S. (2016). Protein-retention expansion microscopy of cells and tissues labeled using standard fluorescent proteins and antibodies. *Nature Biotechnology*, *34*(9), 987–992. https://doi.org/10.1038/nbt.3625

60. Tu, J. C., Xiao, B., Naisbitt, S., Yuan, J. P., Petralia, R. S., Brakeman, P., … Worley, P. F. (1999). Coupling of mGluR/Homer and PSD-95 complexes by the Shank family of postsynaptic density proteins. *Neuron*, *23*(3), 583–592. https://doi.org/10.1016/S0896-6273(00)80810-7

61. Tuchman, R., & Rapin, I. (2002). Epilepsy in autism. *The Lancet. Neurology*, *1*(6), 352–358. https://doi.org/10.1016/S1474-4422(02)00160-6

62. Wang, X., McCoy, P. A., Rodriguiz, R. M., Pan, Y., Je, H. S., Roberts, A. C., … Jiang, Y.-H. (2011). Synaptic dysfunction and abnormal behaviors in mice lacking major isoforms of Shank3. *Human Molecular Genetics*, *20*(15), 3093–3108. https://doi.org/10.1093/hmg/ddr212

63. Wang, X., Zhang, C., Szábo, G., & Sun, Q.-Q. (2013). Distribution of CaMKIIα expression in the brain in vivo, studied by CaMKIIα-GFP mice. *Brain Research*, *1518*, 9–25. https://doi.org/10.1016/j.brainres.2013.04.042

64. Wang, X., Xu, Q., Bey, A. L., Lee, Y., & Jiang, Y. H. (2014). Transcriptional and functional complexity of Shank3 provides a molecular framework to understand the phenotypic heterogeneity of SHANK3 causing autism and Shank3 mutant mice. *Molecular Autism*. https://doi.org/10.1186/2040-2392-5-30

65. Wöhr, M., Roullet, F. I., Hung, A. Y., Sheng, M., & Crawley, J. N. (2011). Communication impairments in mice lacking Shank1: reduced levels of ultrasonic vocalizations and scent marking behavior. *PloS One*, *6*(6), e20631. https://doi.org/10.1371/journal.pone.0020631

66. Won, H., Lee, H.-R., Gee, H. Y., Mah, W., Kim, J.-I., Lee, J., … Kim, E. (2012). Autistic-like social behaviour in Shank2-mutant mice improved by restoring NMDA receptor function. *Nature*, *486*(7402), 261–265. https://doi.org/10.1038/nature11208

67. Xu, J., Ma, H., & Liu, Y. (2017). Stochastic Optical Reconstruction Microscopy (STORM). *Current Protocols in Cytometry*, *81*, 12.46.1-12.46.27. https://doi.org/10.1002/cpcy.23

68. Yang, M., Bozdagi, O., Scattoni, M. L., Wöhr, M., Roullet, F. I., Katz, A. M., … Crawley, J. N. (2012). Reduced excitatory neurotransmission and mild autism-relevant phenotypes in adolescent Shank3 null mutant mice. *The Journal of Neuroscience : The Official Journal of the Society for Neuroscience*, *32*(19), 6525–6541. https://doi.org/10.1523/JNEUROSCI.6107-11.2012

69. Yoshimura, Y., Shinkawa, T., Taoka, M., Kobayashi, K., Isobe, T., & Yamauchi, T. (2002). Identification of protein substrates of Ca(2+)/calmodulin-dependent protein kinase II in the postsynaptic density by protein sequencing and mass spectrometry. *Biochemical and Biophysical Research Communications*, *290*(3), 948–954. https://doi.org/10.1006/bbrc.2001.6320

70. Zambrowicz, B. P., Imamoto, A., Fiering, S., Herzenberg, L. A., Kerr, W. G., & Soriano, P. (1997). Disruption of overlapping transcripts in the ROSA beta geo 26 gene trap strain leads to widespread expression of beta-galactosidase in mouse embryos and hematopoietic cells. *Proceedings of the National Academy of Sciences of the United States of America*, *94*(8), 3789–3794. https://doi.org/10.1073/pnas.94.8.3789

71. Zhao, H., Tu, Z., Xu, H., Yan, S., Yan, H., Zheng, Y., … Zhang, Y. Q. (2017a). Altered neurogenesis and disrupted expression of synaptic proteins in prefrontal cortex of SHANK3-deficient non-human primate. *Cell Research*. https://doi.org/10.1038/cr.2017.95

72. Zhao, Y., Bucur, O., Irshad, H., Chen, F., Weins, A., Stancu, A. L., … Boyden, E. S. (2017b). Nanoscale imaging of clinical specimens using pathology-optimized expansion microscopy. *Nature Biotechnology*, *35*(8), 757–764. https://doi.org/10.1038/nbt.3892

73. Zitzer, H., Hönck, H. H., Bächner, D., Richter, D., & Kreienkamp, H. J. (1999). Somatostatin receptor interacting protein defines a novel family of multidomain proteins present in human and rodent brain. *The Journal of Biological Chemistry*, *274*(46), 32997–33001. https://doi.org/10.1074/jbc.274.46.32997

Acknowledgments

There are a few individuals to whom I want to express my particular gratitude. First I want to thank Prof. Dr. Tobias M. Boeckers. He trusted me with the work he gave me, was always very kind and had a charming way of motivating me. My supervisor Dr. Michael Schoen always found time to help me when I needed help. He was also very kind and never lost his patience when I made mistakes. He has become a friend and I am glad and thankful that he was my supervisor. Dr. Christopher Heise helped me so much during the time when my supervisor was sick and could not come to work. His competence and his passion for science made it possible for me to finish my work within time I had. Dr. Jürgen Bockmann, my second supervisor, always had time for any questions I had. He was a very helpful figure during my time at the institute. Frau Ursula Pika-Hartlaub and Frau Renate Zienecker, laboratory technicians at the laboratory I worked in, were so nice and so helpful. Without their knowledge it would have been a lot more difficult to get along during the work days and without their friendliness it would have been a lot less pleasant too. Thanks must also go to my fellow medical student and laboratory co-worker Anna Nusser. When I started my work at the institute she took a surprising amount of time to show me many of the methods that I needed in order to do my work. Another fellow medical student and friend of mine, Jan Schroeder, also played a role that I am thankful for. He did his Bachelor thesis at the institute and it was because of his fondness of his time there that I even applied to do my thesis there in the first place. All in all, there was not one person in the laboratory who did not at some point help me. The fact that everyone was so helpful toward each other made everything a lot easier. Of course I also want to express my gratitude to my family. They have invested so much time and energy into my education and were always supportive with anything I attempted to do. Without them I might not have managed to go down this path. Not everyone is as lucky as I am to have such a family and I am very thankful for it.